



Tracing soil organic carbon in the lower Amazon River and its tributaries using GDGT distributions and bulk organic matter properties

Jung-Hyun Kim^{a,*}, Claudia Zell^a, Patricia Moreira-Turcq^b, Marcela A.P. Pérez^c,
Gwenaël Abril^d, Jean-Michel Mortillaro^e, Johan W.H. Weijers^f, Tarik Meziane^e,
Jaap S. Sinninghe Damsté^{a,f}

^a NIOZ Royal Netherlands Institute for Sea Research, PO Box 59, 1790 AB Den Burg, Texel, The Netherlands

^b IRD-GET-HYBAM, Centre IRD d'Ile de France, 32, Avenue Henri Varagnat, F-93143 Bondy, France

^c PPGGEO, Universidade Federal do Amazonas-UFAM, Avenida Rodrigo O.J. Ramos, 3000 CEP: 69077-000 Manaus, Brazil

^d UMR-CNRS 5805, EPOC, Université Bordeaux 1, Avenue des Facultés, F-33405 Talence, France

^e UMR-CNRS-IRD-UPMC 7208, BOREA, Département Milieux et Peuplements Aquatiques, MNHN, CP 53, 61 rue Buffon, F-75231 Paris Cedex 05, France

^f Department of Earth Sciences, Utrecht University, PO Box 80.021, 3508 TA Utrecht, The Netherlands

Received 18 November 2011; accepted in revised form 9 May 2012

Abstract

In order to trace the transport of soil organic carbon (OC) in the lower Amazon basin, we investigated the distributions of crenarchaeol and branched glycerol dialkyl glycerol tetraethers (GDGTs) by analyzing riverbed sediments and river suspended particulate matter (SPM) collected in the Solimões-Amazon River mainstem and its tributaries. The Branched and Isoprenoid Tetraether (BIT) index, a proxy for river-transported soil OC into the ocean, was determined from the distributions of these GDGTs. The GDGT-derived parameters were compared with other bulk geochemical data (i.e. C:N ratio and stable carbon isotopic composition). The GDGT-derived and bulk geochemical data indicate that riverine SPM and riverbed sediments in the lower Amazon River and its tributaries are a mixture of C₃ plant-derived soil OC and aquatic-derived OC. The branched GDGTs in the SPM and riverbed sediments did not predominantly originate from the high Andes soils (>2500 m in altitude) as was suggested previously. However, further constraint on the soil source area of branched GDGTs was hampered due to the deficiency of soil data from the lower montane forest areas in the Andes. Our study also revealed seasonal and interannual variation in GDGT composition as well as soil OC discharge, which was closely related to the hydrological cycle. By way of a simple binary mixing model using the flux-weighted BIT values at Óbidos, the last gauging station in the Amazon River, we estimated that 70–80% of the POC pool in the river was derived of soil OC. However, care should be taken to use the BIT index since it showed a non-conservative behaviour along the river continuum due to the aquatic production of crenarchaeol. Further investigation using a continuous sampling strategy following the full hydrological cycle is required to fully understand how soil-derived GDGT signals are transformed in large tropical river systems through their transport pathway to the ocean.

© 2012 Elsevier Ltd. All rights reserved.

* Corresponding author. Tel.: +31 (0)222 369567.

E-mail address: Jung-Hyun.Kim@nioz.nl (J.-H. Kim).

1. INTRODUCTION

As one of the major pathways for the ultimate preservation of terrigenous production, the transfer of organic matter (OM) from land to the ocean via rivers is a key process in the global carbon cycle (Ittekkot and Haake 1990; Degens et al., 1991; Hedges et al., 1992). Hence, the role of rivers in the global carbon cycle is most typically expressed as the fluvial export of total organic carbon (TOC, particulate and dissolved organic carbon; POC and DOC, respectively) from land to the ocean (e.g., Likens et al., 1981). Fluvial transport of TOC represents an estimated flux of 0.4–0.6 PgC yr⁻¹ to the global ocean (Schlesinger and Melack, 1981; Spitzky and Ittekkot, 1991; Ludwig et al., 1996; Lal, 2003). Tropical rivers are thought to be responsible for 45–60% of this flux (Meybeck, 1982; Ludwig et al., 1996), and thus form an important link between terrestrial and marine carbon pools (Quay et al., 1992). The Amazon River, the world's largest river by water flow, is responsible for 8–10% of the global terrestrial OC export to the oceans, with DOC (83%) dominating over POC (17%) (Moreira-Turcq et al., 2003).

Most previous studies (Hedges et al., 1986a; Quay et al., 1992; Martinelli et al., 2003), predominantly based on bulk organic parameters such as the C:N ratio and the stable isotopic composition of OC ($\delta^{13}\text{C}_{\text{OC}}$), and lignin composition, indicated that OC in the Amazon River is predominantly soil-derived. These studies have also found particulate organic matter (POM) compositions to be nearly constant over substantial time periods, distances, hydrologic fluctuations, and size fractions (Hedges et al., 1986a; Quay et al., 1992). In contrast, POM in the St Lawrence River (Canada) was dominated by phytoplanktonic material during warm seasons, and terrestrial detritus during colder periods and storm surges (Barth et al., 1998). In the Sanaga River (Cameroon) and Congo River (Central Africa), POM also varied with discharge, with high proportions derived from C₄ plants in savannas during high discharge periods, and high proportions derived from C₃ plants from the riverbanks during low discharge periods (Mariotti et al., 1991; Bird et al., 1998).

Recently, the Branched and Isoprenoid Tetraether (BIT) index (Hopmans et al., 2004) has been developed to trace soil OC in marine environments. This index is based on the relative abundance of non-isoprenoidal, so-called branched, glycerol dialkyl glycerol tetraethers (GDGTs, Sinninghe Damsté et al., 2000) vs. a structurally related isoprenoid GDGT “crenarchaeol” (Sinninghe Damsté et al., 2002). Branched GDGTs are ubiquitous and dominant in peats (Weijers et al., 2004, 2006a) and soils (Kim et al., 2006, 2010; Weijers et al., 2006b, 2007; Huguet et al., 2010), probably derived from anaerobic (Weijers et al., 2006a,b) and heterotrophic (Pancost and Sinninghe Damsté, 2003; Oppermann et al., 2010; Weijers et al., 2010) bacteria. Recent studies indicated that bacteria from the phylum Acidobacteria are a likely source for these branched GDGTs (Weijers et al., 2009a; Sinninghe Damsté et al., 2011). Crenarchaeol is considered to be the specific membrane-spanning lipid of non-extremophilic Thaumarchaeota (Sinninghe Damsté et al., 2002; Schouten

et al., 2008; Pitcher et al., 2011), formerly known as Group I Crenarchaeota (Spang et al., 2010).

The BIT index has been introduced as a new tool initially for estimating the relative amounts of river-transported terrestrial OC in marine sediments (Hopmans et al., 2004) and later, based on the findings of Weijers et al. (2006b), more specifically as a proxy of river-transported soil OC input (Huguet et al., 2007; Walsh et al., 2008; Kim et al., 2009). Recently, Tierney and Russell (2009) showed that in the Lake Towuti area (Indonesia), the concentrations of branched GDGTs were increased along a soil-riverbed-lake sediment transect. Since their branched GDGT distributions were also significantly different to each other, albeit with high and comparable BIT values, they proposed a potential in-situ production of branched GDGTs in the lake water column and/or water-sediment interface in the river itself in addition to soil erosion. In contrast, Zhu et al. (2011) found that the riverbed sediments from the lower Yangtze River had higher branched GDGT concentrations than the marine sediments from the adjacent East China Sea. This indicated that the branched GDGTs in this river system originated predominantly from soil input. Nonetheless, their branched GDGT distribution patterns did not reflect fully their distribution in catchment soils. This led to a conclusion that branched GDGTs could have been produced in the Yangtze River channel itself, contributing at least partly to the branched GDGT pool in the riverbed sediments. Several recent studies in lacustrine environments (Sinninghe Damsté et al., 2009; Tierney and Russell, 2009; Bechtel et al., 2010; Blaga et al., 2010; Tierney et al., 2010; Tyler et al., 2010; Zink et al., 2010; Loomis et al., 2011; Sun et al., 2011) also indicated that aquatic production of branched GDGTs is likely.

Few studies in large rivers have been conducted with sufficient temporal and/or spatial coverage for adequate assessment of GDGT composition and discharge related to seasonal hydrological changes. Here, we investigated riverbed sediments and suspended particulate matter (SPM) collected in the Solimões-Amazon River mainstem and its main tributaries (Negro, Madeira, and Tapajós) in periods of high and low water discharge in 2005 and 2009. We determined variations in crenarchaeol and branched GDGT concentrations as well as BIT index. The results were subsequently compared with other commonly used proxies for terrestrial OM input such as C:N ratio and $\delta^{13}\text{C}_{\text{OC}}$. The aims of this study were (1) to trace the potential compositional alteration of soil OM along the transport pathway and (2) to quantify the relative contribution of soil-derived OC to POC and its discharge to the ocean. Our results provide a qualitative and quantitative assessment of GDGT sources (soil vs. aquatic) and composition in the Amazon River and its tributaries.

2. MATERIAL AND METHODS

2.1. Study area

The Amazon basin runs about 5000 km from the Atlantic coast to the foot of the Andes (Nores, 2011). The bound-

ary between the lowland Amazonian rain forest and the forest of the eastern slopes of the Andes may be restricted to about 500 m in altitude (Patterson et al., 1998; Nores, 2011). The eastern Andean montane forests may be subdivided into two forest belts: lower montane forests (<2500 m in altitude) and upper montane forests (2500–3500 m in altitude, Young, 1999). Páramo (i.e. high alpine grasslands, bogs, and open meadows) is located in the high elevations between the upper forest line (~3000 m in altitude) and the permanent snow line (~5000 m in altitude).

The Amazon River is formed by the confluence of the Ucayali and Marañón Rivers in Peru (Fig. 1A). In Brazil, the main river is referred to as the Solimões River upstream of its confluence with the Negro River. The Amazon River is the world's largest river with a drainage basin area of $6.1 \times 10^6 \text{ km}^2$ covering about 40% of South America

(Goulding et al., 2003), and a mean annual discharge of $200,000 \text{ m}^3 \text{ s}^{-1}$ at Óbidos, the most downstream gauging station in the Amazon River (Callède et al., 2000). The Amazon River supplies approximately 20% of the total volume of freshwater entering the ocean (Meade et al., 1985; Molinier et al., 1996). The Amazon River also ranks second in terms of particle transport with an annual mean sediment discharge of $800\text{--}1200 \times 10^9 \text{ kg yr}^{-1}$ at Óbidos (Dunne et al., 1998; Martinez et al., 2009). Riverine transport of OC by the Amazon exports $32.7\text{--}34.5 \text{ TgC yr}^{-1}$ to the ocean as measured at the outlet of Óbidos, and thus contributes significantly to the global carbon budget (Moreira-Turcq et al., 2003; Bustillo et al., 2011 and references therein). Rivers within the Amazon drainage basin are traditionally classified according to their colour (Sioli, 1950). White water rivers (e.g., Solimões and Madeira) have high levels

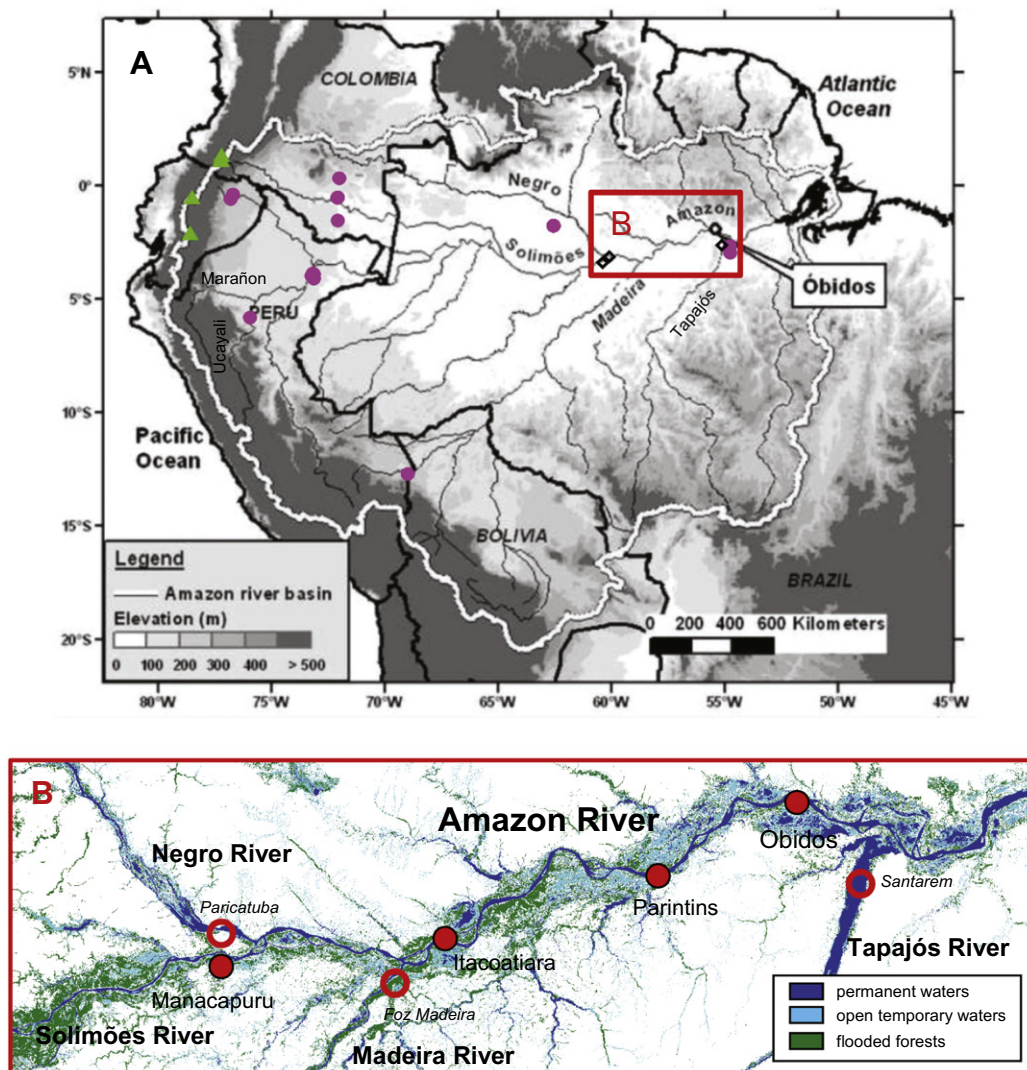


Fig. 1. (A) A general map of the Amazon basin (Martinez et al., 2009) showing the study area (red box) with the sample locations of Andes (>500 m in altitude, filled green triangles) and Amazon (<500 m in altitude, filled purple circles) soils and riverbed sediment (black open diamonds) and (B) a detailed lower Amazon basin map (Martinez and Le Toan, 2007) with river SPM sampling sites on the Amazon River (filled red circles) and its tributaries (open red circles).

of total suspended solids due to the mechanical erosion of the Andean mountain chain (Gibbs, 1967; Meade et al., 1985). The black water rivers (e.g., Negro) originate from lowland regions with bleached sandy soil (podzols) and are characterized by low SPM but high concentrations of dissolved humic substances (Mounier et al., 1998). The clear water rivers (e.g., Tapajós) are depleted in both suspended and dissolved material and often characterized by a high phytoplankton production (Junk, 1997).

2.2. Hydrological data

The daily water levels recorded at Óbidos (1°54.080S, 5°31.1160W) were provided by the Agência Nacional das Águas (ANA). The water level series was described by Callède et al. (2001) and retrieved from the HYBAM project web-site (<http://www.mpl.ird.fr/hybam/>). Water discharge was measured at selected sampling sites with an Acoustic Doppler Current Profiler (ADCP 600 and 1200 Hz, WorkHorse Rio Grande TMRD Instruments) with a precision better than $\pm 5\%$. Water discharge was estimated from at least 4 cross-section measurements with an error of about 5%. Discharges in the Amazon River were computed from the rating curve established for the Óbidos stage. This relationship, initially proposed by Jacon (1987) was improved by Callède et al. (2001) and Filizola and Guyot (2004) using measurements with a 300 and 600 Hz ADCP (WorkHorse Rio Grande TMRD Instruments, Callède et al., 2000).

2.3. Sample collection

Riverbed sediment and river SPM sampling sites are shown in Fig. 1 (see also Table 1). Three surface riverbed sediments were collected using a bottom sediment grab sampler at Paricatuba, Manacapuru, and Óbidos during the December cruise in 2003. River SPM was collected at four mainstem locations (Manacapuru, Itacoatiara, Parintins, Óbidos) on the Solimões-Amazon River and at three of its major tributaries: Negro, Madeira, and Tapajós Rivers (indicated with open circles in Fig. 1B). The water regime of the mainstem of the Solimões-Amazon River is characterized by a monomodal hydrogram with high and low water phases, occurring in May–June and in October–November, respectively (Fig. 2). Therefore, we collected SPM during high and low water periods in 2005 and in 2009 (Fig. 2). Samples were generally collected near the surface. During the 2005 cruises, we also collected SPM along several vertical profiles in the Negro, Solimões, and Amazon Rivers.

All the river SPM samples were collected in a similar way. In brief, about 0.5–5 L of water were collected using a Niskin bottle and filtered onto ashed (450 °C, overnight) and pre-weighed glass fibre filters (Whatman GF-F, 0.7 μm) using a vacuum system, under low pressure. After filtration, the filters were dried either for 24 h at 50 °C or kept frozen on board and freeze-dried after being brought to the lab and then weighed to calculate the concentration of SPM. One part of each filter was used for the elemental and stable isotope analysis. For the GDGT analysis, either the rest of each filter used for the elemental and stable isotope analysis or filters collected separately were used.

2.4. Chemical analyses

2.4.1. Elemental and stable carbon isotope analysis

TOC (or POC) and total nitrogen (TN) of riverbed sediments and river SPM samples were analyzed using an elemental analyzer C-H-N FISOONS NA-2000 at Bondy (France). The average precision on concentration measurements was $\pm 0.1 \text{ mgC g}^{-1}$ for TOC and $\pm 0.05 \text{ mgNg}^{-1}$ for TN. The C:N ratio was calculated as TOC:TN for the riverbed sediments and POC:TN for the river SPM samples. The $\delta^{13}\text{C}_{\text{OC}}$ was analyzed using a Europe Hydra 20–20 mass spectrometer equipped with a continuous flow isotope ratio monitoring (Waterloo University, Canada and University of California, Davis, USA). The $\delta^{13}\text{C}_{\text{OC}}$ values are reported in the standard delta notation relative to Vienna Pee Dee Belemnite (VPDB) standard. The analytical precision (as standard deviation for repeated measurements of the internal standards) for the measurement was 0.06‰ for $\delta^{13}\text{C}_{\text{OC}}$.

2.4.2. Lipid extraction and purification procedure

All samples were processed at NIOZ (The Netherlands). The riverbed sediments and the freeze-dried filters collected in 2005 were ultrasonically extracted with methanol (MeOH, 3 \times), MeOH:dichloromethane (DCM) (1:1 v:v, 3 \times), and DCM (3 \times). The supernatants were combined, the solvents were removed by rotary evaporation, and the extracts were taken up in DCM and dried under a steady stream of pure N_2 .

The freeze-dried filters collected in 2009 were extracted using a modified Bligh and Dyer method (Bligh and Dyer, 1959). Samples were ultrasonically extracted three times for 10 min. using a single-phase solvent mixture of MeOH:DCM:phosphate buffer (8.7 g of K_2HPO_4 in 1 L bidistilled water) 10:5:4 (v:v:v). Upon centrifugation, supernatants were collected and combined. DCM and phosphate buffer were added to the combined extracts to create a new volume ratio of 5:5:4 (v:v:v) and obtain phase separation. The extract (DCM phase) containing the GDGTs was separated from the residue (MeOH–phosphate buffer phase) by centrifugation and collected. The residue phase was extracted twice more with DCM and the combined extracts evaporated to near dryness using a rotary evaporator. The extract was passed over a small column plugged with extracted cotton wool to remove any remaining filter particles and then completely dried under N_2 .

For the quantification of GDGTs, a C_{46} GDGT internal standard was added to two fractions after the total extracts were separated over a small silica gel (activated overnight) column using *n*-hexane:ethyl acetate (1:1, v:v) and MeOH, respectively (2009 SPM samples), or to the total extracts before the extracts were separated into two fractions over an Al_2O_3 (activated for 2 h at 150 °C) column using hexane:DCM (9:1, v:v) and DCM:MeOH (1:1, v:v), respectively (all other samples).

A recent study by Lengger et al. (2012) showed that different extraction and separation techniques for the quantification of core lipid GDGTs gave similar results. Therefore, the two different methods used for quantification of GDGTs in this study provide comparable results.

Table 1

Information on the samples and results of bulk OM and GDGT analyses from riverbed sediments and river SPM samples investigated in this study.

River	Station	Cruise name	Longitude (°)	Latitude (°)	Water discharge (10 ³ m ³ s ⁻¹)	Date (mm/yyyy)	Water depth (m)	Sample name	SPM (mg L ⁻¹)	OC (wt.%)	C:N ratio	δ ¹³ C _{OC} (‰ VPDB)	I (μg g _{OC} ⁻¹)	II (μg g _{OC} ⁻¹)	III (μg g _{OC} ⁻¹)	IV (μg g _{OC} ⁻¹)	BIT
<i>Riverbed sediment</i>																	
Solimões	Manacapuru		-60.553	-3.332		12/2003	Surface	RB-S4		4	11	-28.2	1	0.3	0.04	0.2	0.89
Negro	Paricatuba		-60.263	-3.073		12/2003	Surface	RB-N1		19	16	-27.6	3	0.2	0.01	0.2	0.93
Amazon	Óbidos		-55.302	-1.951		12/2003	Surface	RB-A1		7	10	-28.8	4	1	0.1	0.3	0.94
<i>SPM</i>																	
Solimões	Manacapuru		-60.553	-3.332	125	06/2005	Surface	RS-S1	113	2	8	-28.6	42	8	1.0	6	0.90
					125	06/2005	7	RS-S2	95	2	7	-28.5	37	7	0.8	5	0.90
					125	06/2005	28	RS-S3	121	2	8	-28.4	36	7	0.9	5	0.90
					60	11/2005	Surface	RS-S4	153	1	8	-29.2	50	11	1.5	13	0.83
					60	11/2005	2	RS-S5	189	1	7	-29.3	10	3	0.4	3	0.79
					60	11/2005	8	RS-S6	146	2	8	-28.9	25	5	0.8	11	0.74
					60	11/2005	16	RS-S7	127	2	9	-28.8	34	8	1.1	10	0.81
					60	11/2005	24	RS-S8	215	2	9	-28.7	32	7	1.0	9	0.82
		CBM5			161	06/2009	Surface	CBM502	41	2	8.23	-35.03	81	16	0.0	6	0.94
		CBM6			67	10/2009	Surface	CBM607	74	3	8	-30.2	14	3	0.2	9	0.65
Negro	Paricatuba		-60.263	-3.073	46	05/2005	Surface	RS-N1	6	15	41	-28.5	34	1	0.1	3	0.92
					46	05/2005	10	RS-N2	5	20	30	-29.4	55	2	0.2	5	0.92
					46	05/2005	20	RS-N3	6	16	27	-28.8	68	3	0.2	6	0.92
					46	05/2005	30	RS-N4	8	16	25	-29.0	50	2	0.2	4	0.92
		CBM5			26	06/2009	Surface	CBM514	3	22	11	-31.3	120	9	0.1	11	0.92
		CBM6			30	10/2009	Surface	CBM601	4	23	11	-31.3	53	4	0.2	6	0.90
Madeira	Foz Madeira		-58.790	-3.415	21	06/2005	Surface	RS-M1	53	2	7	-28.0	29	6	0.6	13	0.73
					21	06/2005	23	RS-M2	84	1	7	-27.9	45	9	1.0	19	0.74
					12	11/2005	Surface	RS-M3	172	1	4	-29.2	39	12	1.5	30	0.63
					12	11/2005	3	RS-M4	178	1	5	-29.3	94	29	3.4	51	0.71
					12	11/2005	10	RS-M5	309	1	6	-29.0	27	8	1.1	18	0.67
		CBM5			30	06/2009	Surface	CBM517	53	2	6	-28.5	165	24	1.4	14	0.93
		CBM6			11	10/2009	Surface	CBM621	33	2	6	-29.3	25	7	0.5	37	0.46
Amazon	Itacoatiara		-58.254	-3.093	90	11/2005	Surface	RS-A6	96	1	9	-28.8	54	13	1.7	17	0.80
					90	11/2005	30	RS-A7	107	2	8	-28.9	39	10	1.4	9	0.85
					90	11/2005	62	RS-A8	109	2	8	-28.7	28	6	0.8	12	0.74
		CBM5			n.d.	06/2009	Surface	CBM518	27	4	8	-29.6	152	20	1.0	11	0.94
		CBM6			111	10/2009	Surface	CBM622	23	3	8	-29.3	54	10	0.6	65	0.50
Amazon	Parintins		-56.757	-2.627	192	06/2005	Surface	RS-A2	34	3	9	-29.5	57	7	0.6	15	0.81
					192	11/2005	20	RS-A9	126	1	7	-29.3	46	9	1.1	38	0.60
		CBM5			n.d.	07/2009	Surface	CBM528	24	3	8	-29.7	74	13	0.6	21	0.80
		CBM6			n.d.	10/2009	Surface	CBM634	32	3	7	-29.5	32	6	0.5	51	0.42
Amazon	Óbidos		-55.302	-1.951	194	06/2005	Surface	RS-A3	38	3	11	-28.1	38	6	0.6	12	0.79
					194	06/2005	15	RS-A4	97	2	10	-28.1	35	6	0.6	9	0.82

(continued on next page)

Table 1 (Continued)

River	Station	Cruise name	Longitude (°)	Latitude (°)	Water discharge (10 ³ m ³ s ⁻¹)	Date (mm/yyyy)	Water depth (m)	Sample name	SPM (mg L ⁻¹)	OC (wt.%)	C:N ratio	δ ¹³ C _{oc} (‰ VPDB)	I (μg g _{oc} ⁻¹)	II (μg g _{oc} ⁻¹)	III (μg g _{oc} ⁻¹)	IV (μg g _{oc} ⁻¹)	BIT	
Tapajós	Santarem	CBM5 CBM6	-54.431	-2.242	194	06/2005	45	RS-A5	96	2	10	-27.9	40	7	0.7	10	0.83	
					87	11/2005	Surface	RS-A10	64	2	8	-29.7	49	15	2.4	6	0.67	
					87	11/2005	25	RS-A11	75	3	11	-28.4	6	1	0.2	10	0.44	
					87	11/2005	50	RS-A12	95	2	7	-29.4	18	4	0.6	22	0.51	
					294	07/2009	Surface	CBM531	27	3	8	-29.2	78	13	0.5	17	0.84	
					114	10/2009	Surface	CBM635	31	3	8	-29.3	22	4	0.4	38	0.41	
	Santarem	CBM5 CBM6	-54.431	-2.242	n.d.	06/2005	Surface	RS-Ta1	20	32	6	6	-27.4	4	0.4	0.0	3	0.59
					n.d.	11/2005	Surface	RS-Ta3	5	14	6	-29.6	10	1	0.1	10	0.52	
					n.d.	11/2005	15	RS-Ta4	6	10	5	-29.9	18	3	0.2	19	0.53	
					n.d.	07/2009	Surface	CBM541	3	15	7	-32.9	57	8	0.4	52	0.56	
					n.d.	10/2009	Surface	CBM642	3	22	6	-27.5	9	2	0.2	4	0.74	
					n.d.													

n.d. indicates "not determined".

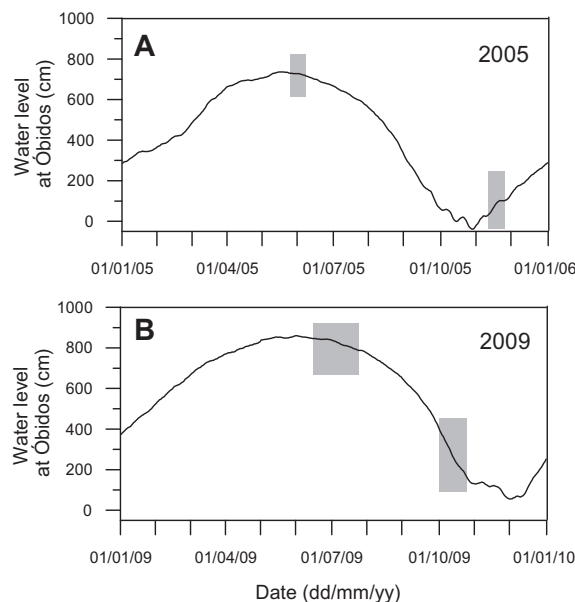


Fig. 2. Variations in water level (cm) at Óbidos, which is the last gauging station in the Amazon River. The grey bars indicate the sampling periods.

2.4.3. GDGT analysis

The GDGT-containing fractions were analyzed at NIOZ (The Netherlands) for GDGTs according to the procedure described by Schouten et al. (2007) with minor modifications. The fractions were dried down under N₂, re-dissolved by sonication (5 min) in *n*-hexane:2-propanol (99:1 v:v) solvent mixture in a concentration of ca. 2 mg ml⁻¹, and filtered through 0.45 μm PTFE filters. The samples were analyzed using high performance liquid chromatography-atmospheric pressure positive ion chemical ionization mass spectrometry (HPLC-APCI-MS). GDGTs were detected by selective ion monitoring of their (M+H)⁺ ions (dwell time 237 ms) and quantification of the GDGT compounds was achieved by integrating the peak areas and using the C₄₆ GDGT internal standard according to Huguet et al. (2006). To correct the potential carryover of GDGTs into the MeOH fraction for the SPM samples collected in 2009, the MeOH fractions were also analyzed using the HPLC-APCI-MS. The BIT index was calculated according to Hopmans et al. (2004):

$$\text{BIT index} = \frac{[\text{I}] + [\text{II}] + [\text{III}]}{[\text{I}] + [\text{II}] + [\text{III}] + [\text{IV}]} \quad (1)$$

[I], [II], and [III] are the concentration of branched GDGTs and [IV] the concentration of isoprenoid GDGT crenarchaeol (Appendix 1). The instrumental reproducibility was determined by triplicate measurements of three samples. The average standard deviation of the BIT index was ±0.002. For the concentration of GDGTs, the analytical errors were ±8% for GDGT I, ±8% for GDGT II, ±12% for GDGT III, and ±9% for crenarchaeol. Note that only tiny amounts of riverbed sediments and SPM, except for those collected during the low water period in 2009, were available for this study, resulting in low total extract yields. As

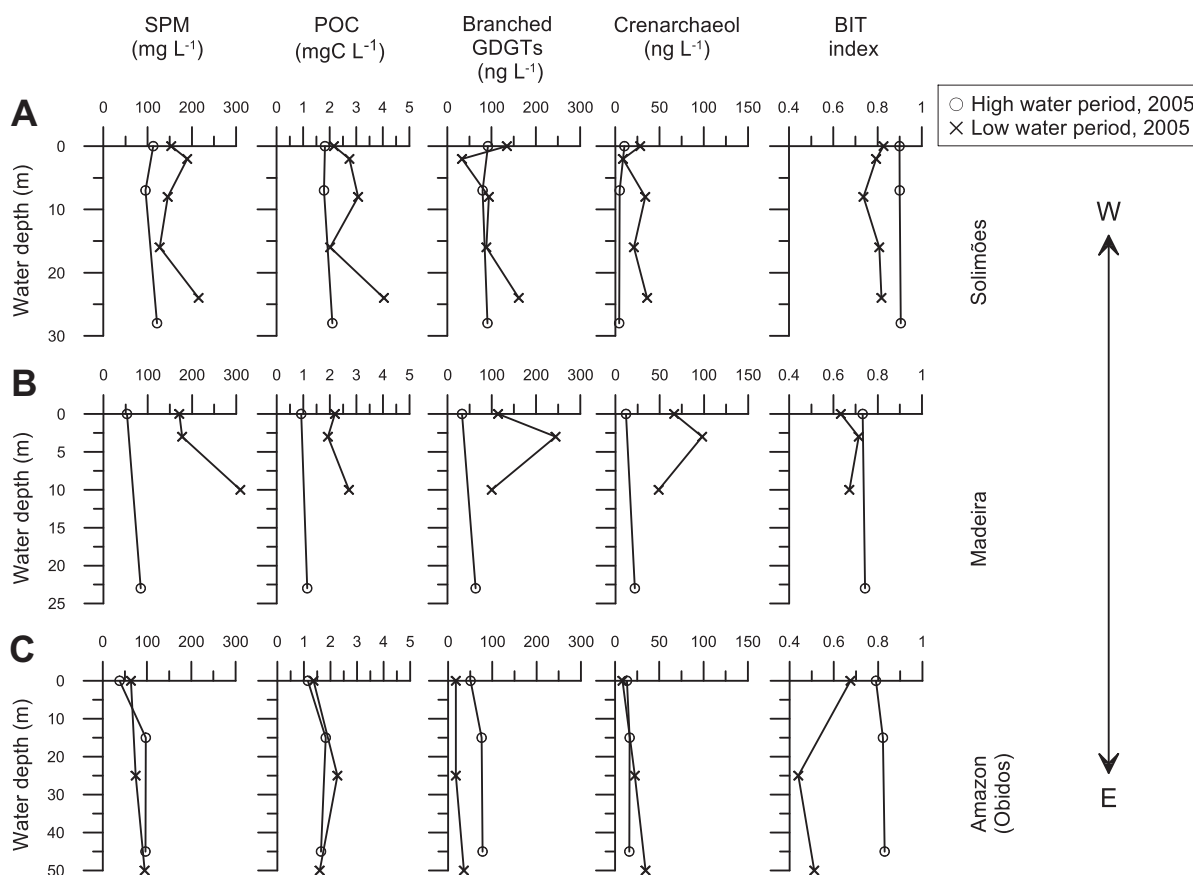


Fig. 3. Water depth profiles of SPM (mg L^{-1}), POC concentration (mg C L^{-1}), sum of branched GDGT concentration (ng L^{-1}), crenarchaeol concentration (ng L^{-1}), and BIT index at (A) Manacapuru (Solimões River), (B) Foz Madeira (Madeira River), and (C) Óbidos (Amazon River).

a consequence, branched GDGTs bearing one or two cyclopentane moieties were below quantification limits. Therefore, we considered only the three major branched GDGT compounds without cyclopentane moieties in this study.

2.5. Statistical analysis

A principal component analysis (PCA) was carried out in order to test the statistical difference between GDGT distributions. We used the fractional abundances (f) of crenarchaeol and branched GDGTs acquired from the riverbed sediments and the river SPM samples in the lower Amazon basin as well as those for Andes and lowland Amazon soils (Appendix 2). The Brodgar v.2.5.2 (<http://www.brodgar.com>) software package was used.

3. RESULTS

3.1. Hydrological data

During the high and low water sampling periods (Fig. 2), the instantaneous water discharge along the mainstem was $125\text{--}194 \times 10^3$ and $60\text{--}87 \times 10^3 \text{ m}^3 \text{ s}^{-1}$ in 2005 and $161\text{--}294 \times 10^3$ and $67\text{--}114 \times 10^3 \text{ m}^3 \text{ s}^{-1}$ in 2009,

respectively (Table 1). During the same periods, the water discharge was $26\text{--}46 \times 10^3$ and $30 \times 10^3 \text{ m}^3 \text{ s}^{-1}$ at the Negro River station, while $21\text{--}30 \times 10^3$ and $11\text{--}12 \times 10^3 \text{ m}^3 \text{ s}^{-1}$ at the Madeira River station. Unfortunately, water discharge measurements were not carried out at the Negro River sampling site in November 2005 and at the Tapajós River sampling sites in both 2005 and 2009.

3.2. Bulk geochemical parameters

3.2.1. River SPM

SPM and POC concentrations as well as other geochemical parameters (C:N ratio and $\delta^{13}\text{C}_{\text{OC}}$) showed little variation with depth for the two stations (Manacapuru and Óbidos) in the Solimões-Amazon River mainstem where this was measured (Fig. 3A and C, Table 1). In general, no consistent trend with depth was observed in any of the parameters measured. For all investigated stations in the Solimões-Amazon River mainstem, the concentrations of surface SPM were lower at times of relatively high water discharge (Fig. 4A) with total SPM concentrations ranging from 23 to 215 mg L^{-1} (Table 1). The OC content of SPM was in the range of 1–4 wt.% (Fig. 5, Table 1) and the POC concentrations varied between 0.8 and 2.3 mg C L^{-1}

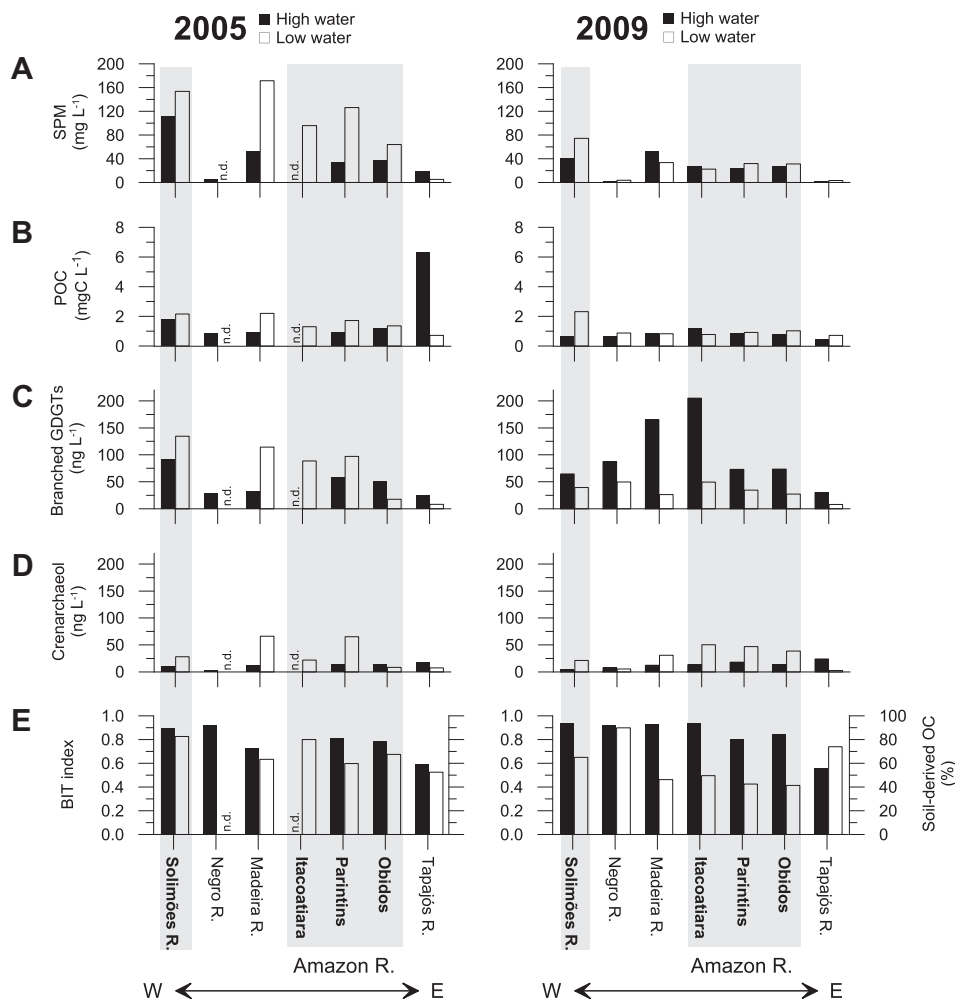


Fig. 4. Concentration in near surface water SPM during high and low water stands (black and white bars, respectively) along a W–E transect of stations in the Solimões–Amazon River (in grey areas) and its tributaries: (A) SPM (mg L^{-1}), (B) POC (mg C L^{-1}), (C) summed branched GDGTs (ng L^{-1}), (D) crenarchaeol (ng L^{-1}), and (E) the BIT index and calculated soil OC percentages. n.d. denotes “not determined”.

(Fig. 4B). The C:N ratio and the $\delta^{13}\text{C}_{\text{OC}}$ fluctuated between 7 and 11 and between -35.0‰ and -27.9‰ , respectively (Fig. 5).

In comparison to the Solimões–Amazon River mainstem, the SPM concentrations were lower in the Negro River, in the range of $4\text{--}6 \text{ mg L}^{-1}$ (Fig. 4A). However, the OC content of SPM was much higher ranging from 15–23 wt.% (Fig. 5, Table 1) and consequently the POC concentration, varying between 0.8 and 0.9 mg C L^{-1} , was of the same order of magnitude in the Solimões–Amazon River mainstem (Fig. 4B). Except for the extremely high C:N ratio values in the 2005 high water period, in general, the C:N ratio (~ 11) and the $\delta^{13}\text{C}_{\text{OC}}$ (-31.3‰ to -28.5‰) were comparable to those along the Solimões–Amazon River mainstem (Fig. 5).

Similar to the water depth profiles of the Solimões–Amazon River mainstem, the water depth profiles of the Madeira River showed no apparent trend with depth for any of the bulk parameters (Fig. 3B, Table 1). In the Madeira River, the SPM concentrations (Fig. 4A) was high during

the low water stage ($\sim 170 \text{ mg L}^{-1}$) compared to the high water period ($\sim 50 \text{ mg L}^{-1}$) in 2005, but this difference was not apparent in 2009 when only relatively small variations were observed ($33\text{--}53 \text{ mg L}^{-1}$, Fig. 4). The OC content of SPM was between 1 and 2 wt.% (Fig. 5, Table 1) and the POC concentration between 0.8 and 2.2 mg C L^{-1} (Fig. 4B), which was comparable to those in the Solimões–Amazon River mainstem. The average values of C:N ratio and $\delta^{13}\text{C}_{\text{OC}}$ were -5.9‰ and -28.7‰ , respectively (Fig. 5), similar to those of the Solimões–Amazon River mainstem.

In the Tapajós River, the SPM concentrations were relatively low (i.e. between 3 and 20 mg L^{-1} , Fig. 4A) similar to those in the Negro River. The OC content of SPM, ranging from 15–32 wt.% (Fig. 5, Table 1), was always high in comparison with those in the Solimões–Amazon River mainstem. The POC concentration was much higher during the 2005 high water period (i.e. 6.3 mg C L^{-1}) than the average of other periods (Fig. 4B). On average, the C:N ratio was 6.3 and the $\delta^{13}\text{C}_{\text{OC}}$ -29.4‰ (Fig. 5).

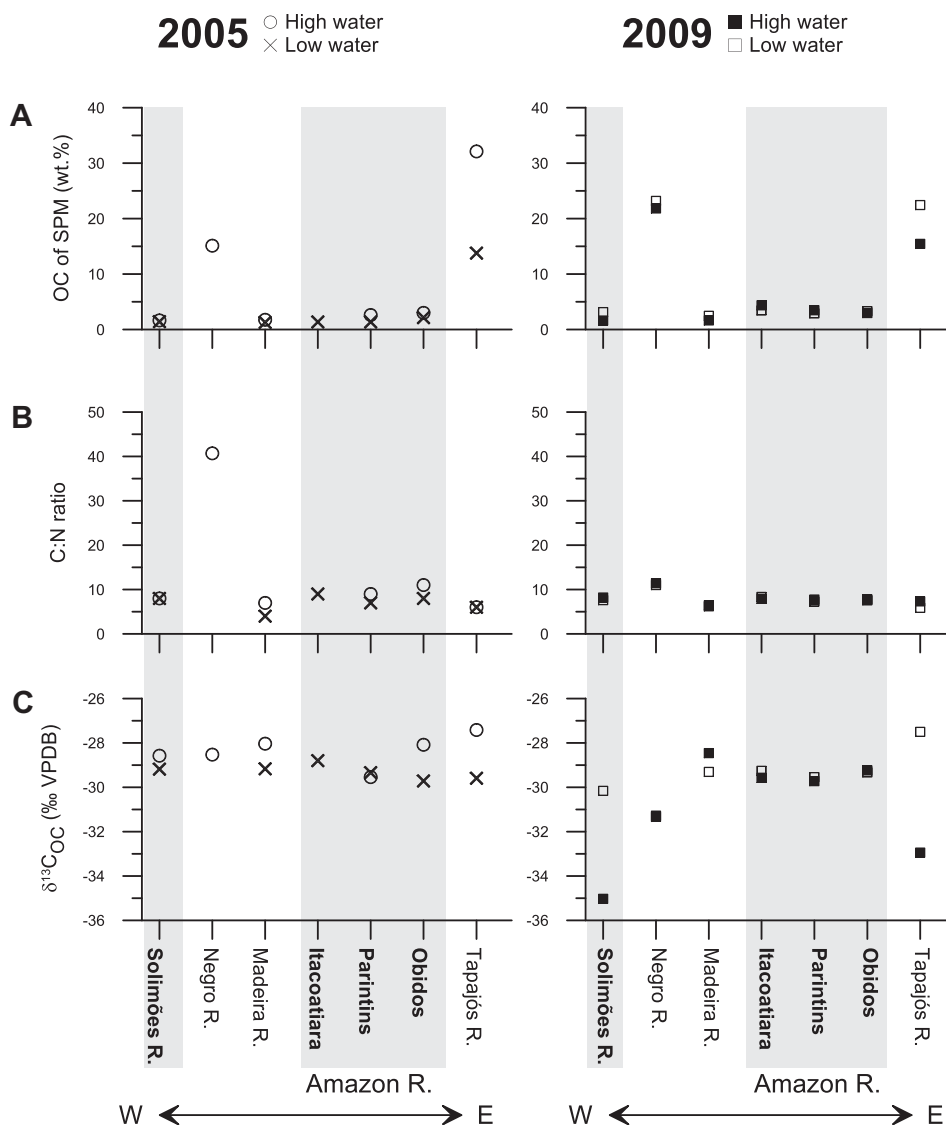


Fig. 5. Downriver trends in (A) OC (wt.%), (B) C:N ratio and (C) $\delta^{13}\text{C}_{\text{OC}}$ (‰ VPDB) of near surface water SPM during high and low water periods along a W–E transect of stations in the Solimões–Amazon River (in grey areas) and its tributaries.

3.2.2. Riverbed sediments

The TOC content of the riverbed sediments was high (4–19 wt.%, Table 1). The C:N ratio varied between 10 and 16 and the $\delta^{13}\text{C}$ value ranged from -28.8‰ to -27.6‰ . For the Negro riverbed sediment, the TOC content and the C:N ratio were much higher than for the Amazon River sediments.

3.3. GDGT parameters

3.3.1. River SPM

Branched GDGTs and crenarchaeol were detected in all river SPM samples and GDGT distributions were dominated by branched GDGT I (Table 1). Water depth profiles of GDGT concentrations and BIT values did not show clear trends in the Solimões–Amazon River (Figs. 3A and C). Along the Solimões–Amazon River mainstem (Fig. 4),

the concentrations of branched GDGTs during the high water season in 2005 were lower ($50\text{--}90\text{ ng L}^{-1}$) than those during the low water season in 2005 ($20\text{--}130\text{ ng L}^{-1}$). In contrast, in 2009, the branched GDGT concentrations were higher during the high water season ($70\text{--}200\text{ ng L}^{-1}$) than during the low water season ($30\text{--}50\text{ ng L}^{-1}$). The concentrations of crenarchaeol varied between 4 and 18 ng L^{-1} during the high water season and between 8 and 70 ng L^{-1} during the low water season. In general, the crenarchaeol concentrations were lower during the high water seasons than during the low water seasons for both 2005 and 2009. It appears that variations in the concentrations of branched GDGTs are larger than those in crenarchaeol along the Solimões–Amazon River mainstem. The BIT index varied between 0.41 and 0.94 with higher values during the high water season than during the low water season. While BIT values during the high water season in 2005

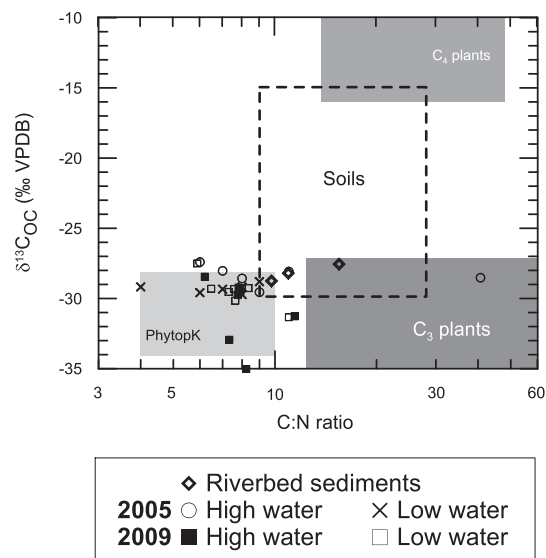


Fig. 6. Scatter plot of $\delta^{13}\text{C}_{\text{OC}}$ (‰ VPDB) vs. the C:N ratio of near surface SPM and riverbed sediments. The boundaries of major OM sources are defined according to Araújo-Lima et al. (1986), Hedges et al. (1986a), Volkoff and Cerri (1987), Martinelli et al. (1994, 2003), Meyers (1994), and Zocatelli (2010). PhytopK indicates phytoplankton.

and 2009 are comparable, those from the low water season in 2005 were higher than those from the low water season in 2009. This suggests that interannual variations in the BIT index are higher for the low water seasons than for the high water seasons.

The concentrations of branched GDGTs and crenarchaeol in the Negro River were of the same order of magnitude compared to those in the Solimões-Amazon River mainstem, and varied between 30 and 90 ng L^{-1} and between 2 and 8 ng L^{-1} , respectively (Fig. 4). The BIT index was constant at ca. 0.90 and showed no significant difference between the high and low water periods in 2009.

Similar to the Solimões-Amazon River mainstem, the concentration profile of GDGTs with water depth did not show clear trends in the Madeira River (Fig. 3B). It appears that the Madeira River behaved similar to the Solimões-Amazon River mainstem, showing that the concentrations of both branched GDGTs and crenarchaeol were higher during the low water period (120 and 70 ng L^{-1} , respectively) than during the high water period (30 and $\sim 10 \text{ ng L}^{-1}$, respectively) in 2005 (Fig. 4). In contrast, the branched GDGT concentrations were elevated during the high water level in 2009, whereas that of crenarchaeol remained similar to that in 2005. The BIT index varied between 0.73 and 0.93.

In the Tapajós River, the concentrations of both branched GDGTs and crenarchaeol obtained from SPM were higher during the high water levels than during the low water levels, ranging from 8 to 30 ng L^{-1} and from 3 to 20 ng L^{-1} , respectively (Fig. 4). In general, lower concentrations of the branched GDGTs in the Tapajós River resulted in lower BIT values than in other rivers. However,

for the low water season in 2009, the crenarchaeol concentration was lower than that for the low water level in 2005, whilst the branched GDGT concentration was virtually the same. This resulted in an opposite pattern, showing higher BIT value during the low water level than during the high water level in 2009 (Fig. 4E).

3.3.2. Riverbed sediments

Branched GDGTs and crenarchaeol were detected in all riverbed sediments investigated. Branched GDGT I was the most abundant GDGT (Table 1). The summed concentrations of branched GDGTs in riverbed sediments ranged between 2 and 5 $\mu\text{g g}_{\text{OC}}^{-1}$, whilst that of crenarchaeol varied between 0.2 and 0.3 $\mu\text{g g}_{\text{OC}}^{-1}$ (Table 1). Since the branched GDGTs were much more abundant than crenarchaeol (about one order of magnitude), the resulting BIT values were high (0.91–0.95) close to the terrestrial theoretical end member value of BIT of 1 (Hopmans et al., 2004).

4. DISCUSSION

4.1. Origin of riverine OM based on bulk geochemical parameters

The C:N ratio and $\delta^{13}\text{C}_{\text{OC}}$ were used as indicator for the origin of the OM of river SPM and the riverbed sediments. Boundaries for these parameters for major OM sources are illustrated in Fig. 6 based on previous studies in the Amazon basin. In the Amazonian forests where most of trees use the Calvin-Benson cycle of carbon fixation (i.e. so-called C_3 plants), $\delta^{13}\text{C}_{\text{OC}}$ of C_3 plants varies between -27‰ and -35‰ (Hedges et al., 1986a; Martinelli et al., 1994, 2003) and the C:N ratio between 13 and 330 (Hedges et al., 1986a; Martinelli et al., 2003). The $\delta^{13}\text{C}_{\text{OC}}$ of the surface soil layer under C_3 plant vegetation ranged from -15‰ to -30‰ (Volkoff and Cerri, 1987) with a C:N ratio of 9–28 (Hedges et al., 1986a; Martinelli et al., 2003). On the other hand, the $\delta^{13}\text{C}_{\text{OC}}$ of C_4 plants (e.g., *Echinochloa polystachya*) was enriched (-9‰ to -16‰) with a C/N ratio of 14–48 (Martinelli et al., 2003; Zocatelli, 2010). Soils under grass (C_4 plant) vegetation were found to have $\delta^{13}\text{C}$ values between -12‰ and -16‰ (Hedges et al., 1986a; Martinelli et al., 2003) and C:N ratio of 18–85 (Martinelli et al., 2003). Phytoplankton and periphyton in the Amazon River system are typically depleted in ^{13}C ($\delta^{13}\text{C}_{\text{OC}} \approx -28\text{‰}$ to -34‰ , Araújo-Lima et al., 1986) similar to C_3 land plants ($\delta^{13}\text{C}_{\text{OC}} \approx -27\text{‰}$ to -35‰ , Hedges et al., 1986a; Martinelli et al., 1994, 2003). Although information on the C:N ratio of phytoplankton in the Amazon River system is lacking, the values for the C:N ratio are expected to be close to the range of C:N ratio for freshwater phytoplankton reported in other freshwater systems (4–10, LaZerte, 1983; Lee and Furhman, 1987; Meyers, 1994).

The C:N ratio of SPM samples and riverbed sediments from the white water (Solimões and Amazon) and clear water (Tapajós) rivers was typically <12 and $\delta^{13}\text{C}_{\text{OC}}$ values were $<-27\text{‰}$ (Fig. 6). The typical range of C:N values for world's riverine POM is ~ 10 – 12 (Meybeck, 1982; Hedges et al., 1986a). Hence, the average C:N ratio of the white and clear water rivers (8 ± 1.5 (mean \pm standard deviation

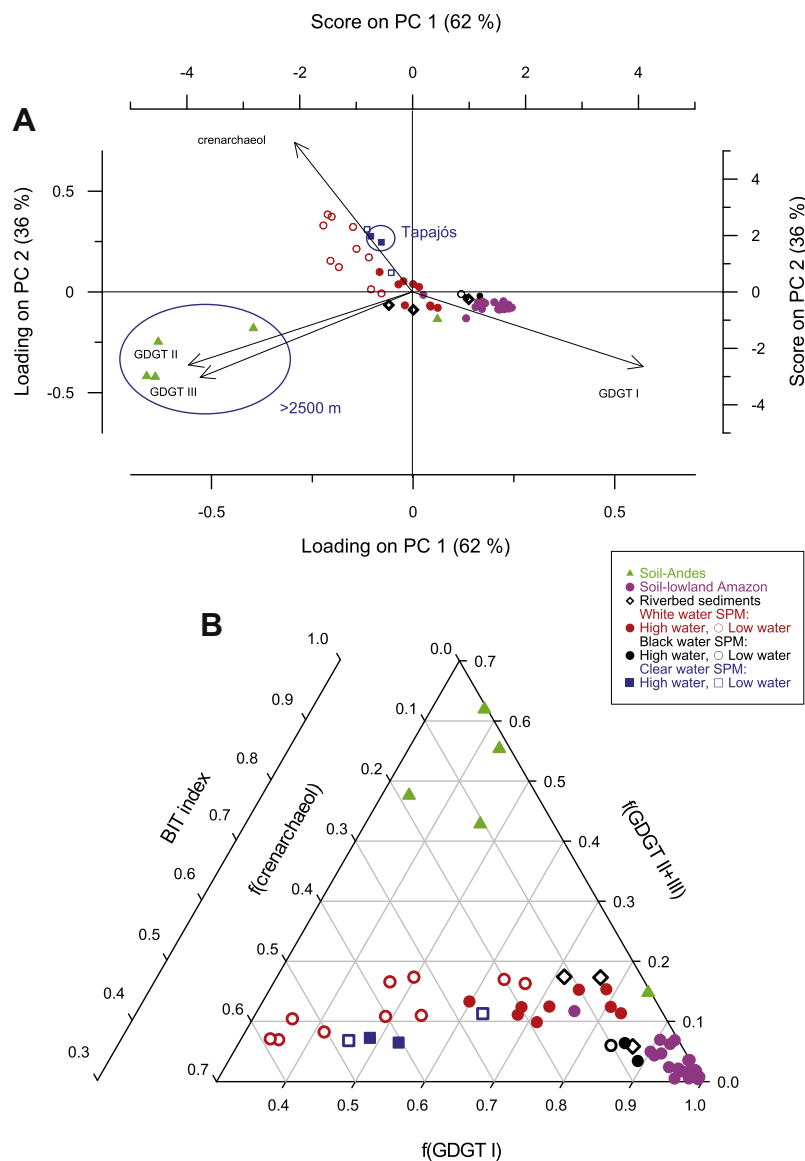


Fig. 7. (A) PCA biplot of the sample scores and the GDGT loadings. Symbols and black lines represent scores of the samples and loadings of the response variables (crenarchaeol and three major branched GDGTs), respectively. (B) Ternary diagram showing the relationships of the fractional abundances (f) of crenarchaeol and three major branched GDGTs. Since GDGT II and GDGT III have similar loadings on the PCA biplot, they were combined for construction of the ternary diagram. Note that $f(\text{crenarchaeol})$ is the same as $(1-\text{BIT})$. A BIT axis has therefore been added to the diagram.

(1σ , $n = 39$) is slightly lower than that of world's riverine POM and the Amazon soil OM. This could be related to the presence of microbial biomass in the river water, which typically has a low C:N ratio, or clay minerals, which can contribute inorganic N lowering C:N ratio (Devol and Hedges, 2001). The SPM and riverbed sediment from the Negro River (black water) collected during the high water period in 2005 differed from the white and clear water rivers as it had a higher C:N ratio (>16 ; Table 1). This suggests that its OM predominantly consists of relatively unaltered vascular plant detritus (Hedges et al., 1986a). Although C_4 aquatic herbaceous macrophytes, such as *Paspalum repens* and *E. polystachya*, are important for the carbon dynamics in the Amazonian floodplains (e.g., Silva et al.,

2009), Hedges et al. (1986a) suggested that only 3% of fine POC in the Solimões-Amazon River mainstem appeared to originate from C_4 plants. This is in good agreement with our $\delta^{13}\text{C}$ data, indicating an insignificant input of C_4 grass in riverine SPM. Mostly low C:N ratios and depleted $\delta^{13}\text{C}$ values (Fig. 6) are indicative of phytoplankton origin, suggesting that aquatic production might be an additional important source to the POC pool of the Solimões-Amazon River mainstem. Based on fatty acid and stable isotope ($\delta^{13}\text{C}_{\text{OC}}$ and $\delta^{15}\text{N}$) analyses, a recent study (Mortillaro et al., 2011) indeed indicated that cyanobacteria and C_3 aquatic plants were important OM sources in the aquatic system in the lower Amazon basin, particularly during the low water season. Taken together, riverine SPM in the low-

er Amazon basin is possibly a mixture of C₃ plant-derived soil OM and aquatic-derived OM.

4.2. Sources of branched GDGTs

Branched GDGTs and crenarchaeol were found in all river SPM and riverbed sediments at varying concentrations (Figs. 3 and 4). The occurrence of branched GDGTs and crenarchaeol has been also reported in SPM of European rivers such as Rhine, Meuse, Niers, and Berkel in the Netherlands (Herfort et al., 2006) as well as Têt and Rhône in France (Kim et al., 2007). The identification of branched GDGTs in the lower Amazon River and its tributaries is consistent with their presence in the Andes and lowland Amazon soils (Bendle et al., 2010; Huguet et al., 2010), and fits the hypothesis that erosion of soil and transport by rivers is an important mechanism for the delivery of branched GDGTs to coastal marine sediments (Hopmans et al., 2004).

To examine the sources of river-transported branched GDGTs, we compared the distribution pattern of the river SPM and the riverbed sediments in the lower Amazon basin with those of the Andes and lowland Amazon soils (Bendle et al., 2010; Huguet et al., 2010; Appendix 2) by performing principal component analysis (PCA) using the fractional abundances (*f*) of crenarchaeol and branched GDGTs. The PCA biplot of the sample scores and the GDGT loadings (Fig. 7A) shows that the first two PCA components (PC1 and PC2) explain 98% of the variation of the GDGT data. On the PC1 axis (explaining 62% of the variance), GDGT I ($r = 0.6$) is negatively correlated with GDGT II and GDGT III ($r = -0.6$ and $r = -0.5$, respectively). On the PC2 axis (explaining 37% of the variance), crenarchaeol ($r = 0.7$) is negatively correlated with all branched GDGTs ($r = -0.4$).

In the PCA, four of the five soils from the high Andes, i.e. from the upper montane forests and páramo vegetation belts (>2500 m in altitude; Appendix 2), cluster as a distinct group in the lower left quadrant of the biplot and are clearly separated from the lowland Amazon soils (<500 m in altitude; Appendix 2) in the lower right quadrant of the biplot. The same pattern is observed in a ternary diagram plotting $f(\text{crenarchaeol})$, $f(\text{GDGT I})$, and $f(\text{GDGT II+III})$ (Fig. 7B). The distribution of branched GDGTs in the high Andes soils is different from that in the lowland Amazon soils with roughly equal amounts of branched GDGT I and II (Appendix 2). Changes in the branched GDGT distribution in soils have been attributed to the adaptation of branched-GDGT producing bacteria to temperature for maintaining an acceptable degree of the membrane fluidity at different temperatures by varying the relative abundance of additional methyl groups (Weijers et al., 2007). Higher proportions of GDGT II (containing five instead of four methyl groups in comparison with GDGT I) in the high Andes soils is thus consistent with the higher altitude and, consequently, lower mean annual air temperature (Bendle et al., 2010). On the other hand, all lowland Amazon soils cluster together (Fig. 7) despite their widespread geographical origin (Appendix 2) since

variation in the mean annual air temperature is small in the lowland Amazon basin (New et al., 2002).

In general, the river SPM clusters well apart from the high Andes soils (Fig. 7), indicating that the branched GDGTs in river SPM did not predominantly originate from the high Andes soils as suggested previously (Bendle et al., 2010). The distribution of branched GDGTs in the riverbed sediments did also not reflect that of the high Andes soils, excluding a predominant Andean source (Fig. 7). The branched GDGT distribution in the riverine SPM and the riverbed sediment from the black water (Negro) river, which does not receive any Andes material (Fig. 1), resembled the branched GDGT distribution in the lowland Amazon soils to the largest extent. Its score on PC1 (Fig. 7B) reflects that the branched GDGT distribution is identical to that of the lowland Amazon soils, suggesting that the branched GDGTs in SPM are predominantly derived from the erosion of lowland soils. The other SPM samples exhibit lower scores on PC1 (Fig. 7A), which could mean that soils in the Andes play a more prominent role as a source for the branched GDGTs in SPM. However, the score on PC1 of the clear water SPM from the Tapajós river, which does not contain any Andes material like the black water river (Fig. 1), is approximately the same as the average score of all white water SPM samples and clearly distinct from that of the black water SPM and the lowland Amazon soils (Fig. 7A). This suggests that, in addition to the soil erosion, aquatic production may contribute at least partly to the riverine branched GDGT pool, and modifies the distribution of branched GDGTs in such a way that it contains higher fractional abundances of GDGT II. Other studies have already suggested that aquatic production of branched GDGTs is probable in river and lacustrine environments (Sinninghe Damsté et al., 2009; Tierney and Russell, 2009; Bechtel et al., 2010; Blaga et al., 2010; Tierney et al., 2010; Tyler et al., 2010; Zink et al., 2010; Loomis et al., 2011; Sun et al., 2011; Zhu et al., 2011). Our results can thus be explained by a mixed soil-derived/aquatic source for the riverine branched GDGTs. However, it is still difficult to quantitatively disentangle the source (soil vs. aquatic) of branched GDGTs in the Solimões-Amazon mainstem, in part due to the deficiency of soil data from the lower montane forest vegetation belt (500–2500 m in altitude) in the Andes. An extended soil data set with a broader spatial coverage of the Andes as well as the lowland Amazon basin could certainly assist in solving this issue. In addition to the distributional and concentration (which are also lacking for the Amazon River system) data from soils, studies on intact polar lipids, i.e. lipids that still contain a polar head group and presumably are derived from living cells, may shed more light on the source identification of the branched GDGTs along the Solimões-Amazon mainstem.

4.3. Riverine crenarchaeol production: consequences for the BIT index

Due to the presence of crenarchaeol in the Andes and lowland Amazon soils, albeit in relatively low amounts

(Appendix 1), the average BIT value (0.97) is slightly lower than the hypothetical terrestrial end-member value of 1 (Hopmans et al., 2004). The BIT indices of the riverine SPM revealed large variation in time and space in Amazonian rivers, but is generally (i.e. 0.4–0.9) lower than the BIT values of the Andes and lowland Amazon soils (Figs. 4 and 7B). This is rather different from the high mountainous, small Têt River (France), where BIT values hardly varied and fitted the average BIT value of soils in the catchment area (Kim et al., 2007, 2010). This indicated that the source of GDGTs to the Têt River remained the same and supported the use of the BIT index as a proxy for soil OM input to aquatic environments (e.g., Hopmans et al., 2004). However, a quite different situation is apparent for the Amazon River system.

The BIT values of the white water river SPM were substantially lower during the low water periods than during the high water periods, whereas this trend was not apparent for the clear and black water SPM (Fig. 7B). On the PCA biplot (Fig. 7A), most of the white water river SPM collected during the low water periods plots in the upper left quadrant due to its high score on PC2, reflecting the relative abundance of crenarchaeol, clearly distinct from the position of the other SPM samples. Hence, it seems likely that besides minor amount of soil-derived crenarchaeol, aquatic-derived crenarchaeol produced in the river itself and/or potentially in the floodplain lakes ('várzea') that are part of the Amazon River system is the main source of crenarchaeol for the white water river SPM, predominantly during the low water season. Indeed, there are reports on the presence and growth of Thaumarchaeota, the source organisms for crenarchaeol (e.g., Pitcher et al., 2011), in rivers (Crump and Baross, 2000; Herfort et al., 2009). Interestingly, the clear water SPM collected during the high water periods also plots in the upper left quadrant of the PCA biplot. This suggests that the aquatic production of crenarchaeol may preferentially occur in settings where both suspended and dissolved material is depleted with a high phytoplankton production. This would be consistent with the physiology of Thaumarchaeota since, as nitrifiers, they would depend on the production of fresh OM from which, upon mineralisation, ammonium is formed.

The BIT index in SPM is significantly correlated with the crenarchaeol concentration normalized on OC ($r^2 = -0.43$, $p < 0.0001$) but, to a much lesser degree, with the branched GDGT normalized on OC ($r^2 = 0.13$, $p = 0.013$). This indicates that variations in the BIT index predominantly reflect variation in riverine crenarchaeol production rather than the soil-derived branched GDGT flux. Similar conclusions have been made in the studies of the Congo Fan (Weijers et al., 2009b) and of African lakes (Tierney et al., 2010). Only when the crenarchaeol concentration is representative for aquatic production in the river, the BIT index reflects the contribution of soil-derived POC in SPM. Taken together with the potential aquatic production of branched GDGTs, care should be taken to use the BIT index as a proxy of river-transported soil OC input.

The average BIT value of the riverbed sediments (0.92) is higher than that of SPM (0.73), but somewhat lower than that of the soils (0.97) considered in this study. This sug-

gests that the riverbed sediments also contain aquatic-derived crenarchaeol in addition to soil-derived crenarchaeol but that during settling of riverine SPM alteration of the GDGT profile takes place, probably by selective degradation of crenarchaeol relative to the branched GDGTs (cf. Huguet et al., 2008). However, this hypothesis should be further explored based on more extensive characterization of GDGT distributions in soils as well as riverbank and riverbed sediments, considering that we investigated only three riverbed sediments in this study.

4.4. Variation in discharge of SPM, POC, and GDGTs

The bulk (SPM and POC) and molecular (branched GDGTs and crenarchaeol) concentrations in river water were highly variable among the investigated rivers and seasons (Fig. 4). To estimate the impact of tributary input to the Solimões-Amazon River mainstem, we calculated instantaneous fluxes of SPM, POC, crenarchaeol, and branched GDGTs obtained by multiplying the measured water discharge by the corresponding concentration at each station (Fig. 8). In general, the SPM and POC discharge was positively related to the water discharge, i.e. high SPM flux at high water discharge and vice versa. Exceptions were at Parintins on the Solimões-Amazon River mainstem and at the station of the Madeira River in 2005, where SPM and POC fluxes were higher during the low water discharge than during the high water discharge.

The comparison between the branched GDGT discharge and the water discharge also showed a positive relationship comparable to those observed for SPM and POC. However, the crenarchaeol discharge was lower when the river water discharge was higher, which differs from a previous study carried out in a small, mountainous catchment area, the Têt River system, France (Kim et al., 2007). The Solimões River was always the principal contributor for branched GDGTs to the Amazon River (Fig. 8). The inflow of branched GDGTs from the Solimões River and the outflow at Óbidos were virtually the same, except for the 2009 high water season (Fig. 8). This suggests that generally the loss of branched GDGTs between the mouth of the Solimões River and the Amazon River at Óbidos by degradation and sedimentation processes was compensated by the supply from the Negro and Madeira Rivers and in-situ production. During the high water period in 2009, however, the branched GDGT discharge at Óbidos was twice as high as at the mouth of the Solimões River. The branched GDGT discharge of the Negro and Madeira Rivers increased two and seven fold, respectively, from the low to high water season but the branched GDGT discharge from these tributaries still accounted only for 34% of the total branched GDGT discharge at Óbidos. Given that the branched GDGT discharge from the Solimões River was 48% of that at Óbidos, there is still a missing source for branched GDGTs, probably in-situ production in rivers and/or floodplain lakes.

In contrast, the crenarchaeol discharge at Óbidos was always substantially higher than that at the mouth of Solimões River, which delivered only 20–50% of the total crenarchaeol pool at Óbidos depending on the season

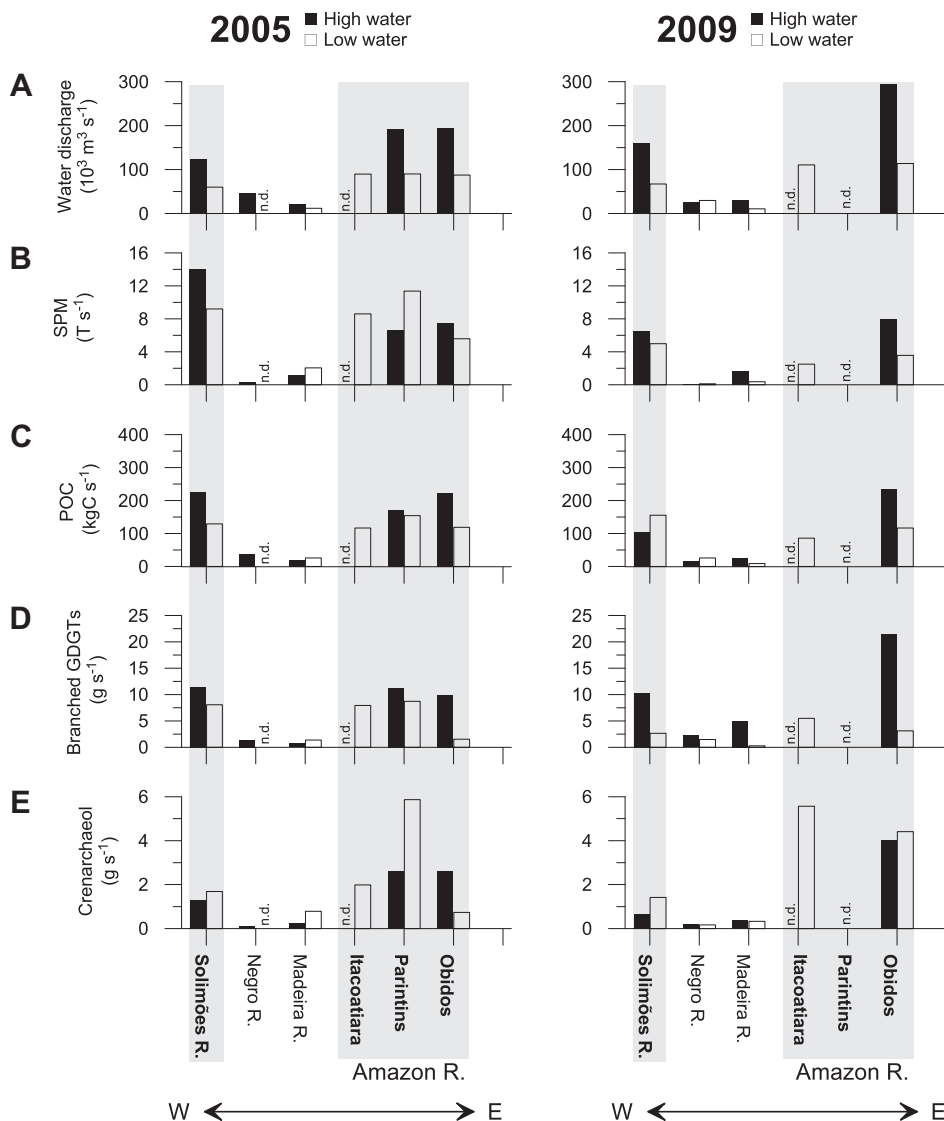


Fig. 8. Comparisons of (A) river water discharge ($\text{m}^3 \text{s}^{-1}$) with (B) SPM discharge (T s^{-1}), (C) POC discharge (kgC s^{-1}), (D) branched GDGT discharge (g s^{-1}), and (E) crenarchaeol discharge (g s^{-1}) during high and low water periods (black and white bars, respectively) along a W–E transect of stations in the Solimões–Amazon River (in grey areas) and its tributaries. To compare the discharge data between 2005 and 2009, we considered only near surface data in 2005. n.d. denotes “not determined”.

(Fig. 8). The crenarchaeol input from the Negro and Madeira Rivers could only account for 10–20% of the crenarchaeol discharge at Óbidos. One viable explanation for this missing source is the aquatic production in the river system (see above) and/or the floodplain lakes, contributing 40–60% of the crenarchaeol discharge at Óbidos.

4.5. Estimation of riverine aquatic and soil OC transport

The BIT values of the Solimões–Amazon River mainstem at Óbidos were variable through time with the mean BIT values of 0.73 for 2005 and 0.63 for 2009. However, the range of the flux-weighted BIT values was smaller with higher values of 0.75 for 2005 and 0.70 for 2009. A binary mixing model based on the BIT index assumes a linear mixing line between the end-members of the BIT index. How-

ever, when two end-members with vastly different mass ratio of components are mixed, the resulting mixing line is not linear. Nevertheless, a study in the NW Mediterranean (Kim et al., 2010) showed that the mass-normalized mixing model resulted in almost identical estimates of soil OC contribution to TOC compared to those based on the BIT values. Hence, we applied a simple binary mixing model based on the flux-weighted BIT values at Óbidos to estimate the portions of aquatic and soil OC to POC as follows:

$$f_{so} = \frac{[\text{BIT}_{\text{sample}}] - [\text{BIT}_{\text{aq}}]}{[\text{BIT}_{\text{so}}] - [\text{BIT}_{\text{aq}}]} \times 100\% \quad (2)$$

where f_{so} is the soil OC fraction and $\text{BIT}_{\text{sample}}$ is the BIT value of the sample investigated. Thereby, we assumed that soil (BIT_{so}) and aquatic (BIT_{aq}) OC end-members are

0.97 (the average value of soils, Appendix 2) and 0.0, respectively. The estimated contributions of soil OC were 78% for 2005 and 73% for 2009, slightly lower than the previous estimation based on the lignin content in the downstream part of the Amazon River (Hedges et al., 1986a).

The annual mean POC discharge at Óbidos is $5.8 \pm 0.3 \text{ TgC yr}^{-1}$ (Moreira-Turcq et al., 2003). When conservatively calculating the portion of the soil OC discharge to POC discharge at Óbidos based on the flux-weighted BIT-derived estimations (73–78%), this would account for $4.2\text{--}4.5 \text{ TgC yr}^{-1}$. Given that in-situ production of branched GDGTs in the aquatic system is possible, this estimation should be considered as high-end values of soil OC percentages to POC. Nonetheless, this supports previous studies based on the lignin composition of POC, which suggested that most of POC in the Amazon River was of a refractory nature and the product of extensive soil degradation (Ertel et al., 1986; Hedges et al., 1986a).

Intensive degradation processes occurring in soils are the principal factors responsible for the relatively refractory material that composes most of the OC flux in the Amazon River (Hedges et al., 1986a). Ittekkot (1988) estimated that only 15% of the POC in high-sediment loaded rivers was generally potentially labile. Our results suggest that the labile component may be larger (i.e. up to 30%) in the Amazon River, if we assume that aquatic-derived OC is more labile than soil-derived OC. If we consider the aquatic production of branched GDGTs and thus a higher BIT index end-member value for the aquatic source, the relative contribution of soil OC to POC might be even lower. Based on the carbon isotope composition (^{13}C and ^{14}C), it has been reported that bulk OC fractions transported by the Amazonian rivers to the ocean range from tens to thousands of years in age (Hedges et al., 1986b; Raymond and Bauer, 2001; Mayorga et al., 2005). Our study implies that the age of riverine OC can vary significantly depending on the contribution of more labile aquatic-derived OC from the river to the ocean. This aspect should be addressed in future studies.

5. CONCLUSIONS

Bulk geochemical data obtained from the downstream part of the Solimões-Amazon River indicated that in-situ (autochthonous) produced OC in the aquatic system is probably an important source to the riverine POC pool. The BIT values were lower in SPM than in soils, especially during the low water periods, indicating in-situ production of crenarchaeol in the aquatic system. Hence, consistent with bulk geochemical data, the distribution patterns of GDGTs reflected a combined effect of soil- and aquatic-derived OC input to the Solimões-Amazon River mainstem. A variable input of aquatic-produced crenarchaeol to the Solimões-Amazon River mainstem, coupled with hydrological changes, was largely responsible for both seasonal and interannual variations in GDGT composition and for variations in soil OC discharge estimates based on the BIT index. Clearly, future work should also focus on intact polar lipids that presumably are derived from living cells, which will help further to provide more direct evidence of

in-situ production of crenarchaeol and branched GDGTs in aquatic settings (river itself and/or floodplain lakes). It should also be noted that care should be taken to use the BIT index for the calculation of the proportion of soil OC to POC, given that the aquatic end-member might be affected by aquatic production of branched GDGTs in the Amazon River system and that the BIT index reflects variations in crenarchaeol concentration rather than soil GDGT flux. Our ‘snapshot’ SPM samples probably did not capture the complete annual variations in GDGT composition and discharge. Therefore, a continuous sampling approach following the full hydrological cycle is required to constrain the effect of hydrological variations on aquatic production of GDGTs and its influence on the use of BIT index as a proxy to trace soil OC input to the ocean.

ACKNOWLEDGEMENTS

We would like to thank J. Ossebaar at NIOZ for analytical support. The research leading to these results has received funding from the European Research Council under the European Union’s Seventh Framework Programme (FP7/2007-2013)/ERC grant agreement n° [226600]. This study was also partly supported by a Marie Curie European Reintegration Grants (ERG) grant to JHK. This work is a part of the CARBAMA project, funded by the ANR, French national agency for research and was conducted within an international cooperation agreement between the CNPq (National Council for Scientific and Technological Development-Brazil) and the IRD (Institute for Research and Development-France). We thank G. Cochonneau and ORG-HYBAM for the water level and river discharge data. We also thank G. Boaventura from the University of Brasilia and P. Seyler from IRD for administrative facilities.

APPENDIX A. SUPPLEMENTARY DATA

Supplementary data associated with this article can be found, in the online version, at <http://dx.doi.org/10.1016/j.gca.2012.05.014>.

REFERENCES

- Araújo-Lima C. A. R. M., Forsberg B. R., Victoria R. and Martinelli L. (1986) Energy sources for detritivorous fishes in the Amazon. *Science* **234**, 1256–1258.
- Barth J. A. C., Veizer J. and Mayer B. (1998) Origin of particulate organic carbon in the upper St. Lawrence. isotopic constraint. *Earth Plan. Sci. Lett.* **162**, 111–121.
- Bechtel A., Smittenberg R. H., Bernasconi S. M. and Schubert C. J. (2010) Distribution of branched and isoprenoid tetraether lipids in an oligotrophic and a eutrophic Swiss lake: insights into sources and GDGT-based proxies. *Org. Geochem.* **41**, 822–832.
- Bendle J. A., Weijers J. W. H., Maslin M. A., Sinninghe Damsté J. S., Schouten S., Hopmans E. C., Boot C. S. and Pancost R. D. (2010) Major changes in glacial and Holocene terrestrial temperatures and sources of organic carbon recorded in the Amazon fan by tetraether lipids. *Geochem. Geophys. Geosyst.* **11**, Q12007. <http://dx.doi.org/10.1029/2010GC003308>.
- Bird M. I., Giresse P. and Ngos S. (1998) A seasonal cycle in the carbon-isotopic composition of organic carbon in the Sanaga River. *Cameroon. Limnol. Oceanogr.* **43**, 143–146.

- Blaga C. I., Reichart G. J., Schouten S., Lotter A. F., Werne J. P., Kosten S., Mazzeo N., Lacerot G. and Sinninghe Damsté J. S. (2010) Branched glycerol dialkyl glycerol tetraethers in lake sediments: can they be used as temperature and pH proxies? *Org. Geochem.* **41**, 1225–1234.
- Bligh E. G. and Dyer W. J. (1959) A rapid method of total lipid extraction and purification. *Can. J. Biochem. Physiol.* **37**, 911–917.
- Bustillo V., Victoria R. L., de Moura J. M. S., de Castro Victoria D., Toledo A. M. A. and Collicchio E. (2011) Factors driving the biogeochemical budget of the Amazon River and its statistical modelling. *Comptes Rendus Geosci.* **343**, 261–277.
- Callède J., Kosuth P., Guyot J.-L. and Guimarães V. (2000) Discharge determination by acoustic Doppler current profilers (ADCP): a moving bottom error correction method and its application on the river Amazon at Óbidos. *Hydrol. Sci. J.* **45**(6), 911–924.
- Callède J., Kosuth P. and Oliveira E. (2001) Etablissement de la relation hauteur-débit de l'Amazone à Óbidos: méthode de la dénivelée normale à géométrie variable. *Hydrol. Sci. J.* **46**, 451–463.
- Crump B. C. and Baross J. A. (2000) Archaeoplankton in the Columbia River, its estuary and the adjacent coastal ocean, USA. *FEMS Microbiol. Ecol.* **31**, 231–239.
- Degens E. T., Kempe S. and Richey J. E. (1991) Chapter 15, summary: biogeochemistry of major world rivers. In: *Biogeochemistry of major world river* (eds. E. T. Degens, S. Kempe and J. E. Richey). Scope 42, Wiley, New York. pp. 323–344.
- Dunne T., Mertes L. A. K., Meade R. H., Richey J. E. and Forsberg B. R. (1998) Exchanges of sediment between the flood plain and channel of the Amazon River in Brazil. *Geol. Soc. Am. Bull.* **110**, 450–467.
- Devol A. H. and Hedges J. I. (2001) Organic matter and nutrients in the mainstem Amazon River. In *The Biogeochemistry of the Amazon Basin* (eds. M. E. McClain, R. L. Victoria and J. E. Richey). Oxford University Press, Oxford, pp. 275–306.
- Ertel J. R., Hedges J. I., Devol A. H., Richey J. E. and Ribeiro M. (1986) Dissolved humic substances of the Amazon River system. *Limnol. Oceanogr.* **31**, 739–754.
- Filizola N. and Guyot J. L. (2004) The use of Doppler technology for suspended sediment discharge determinations in the River Amazon. *Hydrol. Sci. J.* **49**, 143–153.
- Gibbs R. J. (1967) Amazon River system: environmental factors that control its dissolved and suspended load. *Science* **156**, 1734–1737.
- Goulding M., Barthem R. and Ferreira E. (2003) *The Smithsonian Atlas of the Amazon*. Smithsonian Institution Press, Washington, D.C., USA.
- Hedges J. I., Clark W. A., Quay P. D., Richey J. E., Devol A. H. and Santos U. M. (1986a) Composition and fluxes of organic matter in the Amazon River. *Limnol. Oceanogr.* **31**, 717–738.
- Hedges J. I., Quay P. D., Grootes P. M., Richey J. E., Devol A. H., Farwell G. W., Schmidt F. W. and Salati E. (1986b) Organic carbon-14 in the Amazon River system. *Science* **231**, 1129–1131.
- Hedges J. I., Hatcher P. G., Ertel J. R. and Meyers-Schulte K. J. (1992) A comparison of dissolved humic substances from seawater with Amazon River counterparts by ¹³C-NMR spectrometry. *Geochim. Cosmochim. Acta* **56**, 1753–1757.
- Herfort L., Schouten S., Boon J. P., Woltering M., Baas M., Weijers J. W. H. and Sinninghe Damsté J. S. (2006) Characterization of transport and deposition of terrestrial organic matter in the southern North Sea using the BIT index. *Limnol. Oceanogr.* **51**, 2196–2205.
- Herfort L., Kim J.-H., Abbas B., Schouten S., Coolen M. J. L., Herndl G. J. and Sinninghe Damsté J. S. (2009) Diversity of Archaea and potential for crenarchaeotal nitrification of group 1.1a in the rivers Rhine and Têt. *Aquat. Microbial Ecol.* **55**, 189–201.
- Hopmans E. C., Weijers J. W. H., Schefuß E., Herfort L., Sinninghe Damsté J. S. and Schouten S. (2004) A novel proxy for terrestrial organic matter in sediments based on branched and isoprenoid tetraether lipids. *Earth Plan. Sci. Lett.* **224**, 107–116.
- Huguet C., Hopmans E. C., Febo-Ayala W., Thompson D. H., Sinninghe Damsté J. S. and Schouten S. (2006) An improved method to determine the absolute abundance of glycerol dibiphytanyl glycerol tetraether lipids. *Org. Geochem.* **37**, 1036–1041.
- Huguet C., Smittenberg R. H., Boer W., Sinninghe Damsté J. S. and Schouten S. (2007) Twentieth century proxy records of temperature and soil organic matter input in the Drammensfjord, southern Norway. *Org. Geochem.* **38**, 1838–1849.
- Huguet C., de Lange G. J., Gustafsson O., Middelburg J. J., Sinninghe Damsté J. S. and Schouten S. (2008) Selective preservation of soil organic matter in oxidized marine sediments (Madeira Abyssal Plain). *Geochim. Cosmochim. Acta* **72**, 6061–6068.
- Huguet A., Fosse C., Metzger P., Fritsch E. and Derenne S. (2010) Occurrence and distribution of extractable glycerol dialkyl glycerol tetraethers in podzols. *Org. Geochem.* **41**, 291–301.
- Ittekkot V. (1988) Global trends in the nature of organic matter in river suspensions. *Nature* **332**, 436–438.
- Ittekkot V. and Haake B. (1990) The terrestrial link in the removal of organic carbon in Facets of Modern Biogeochemistry. (eds. V. Ittekkot et al.). Springer, New York. pp. 319–325.
- Jaccon G. (1987) Jaugeage de l'Amazone à Obidos par les méthodes du bateau mobile et des grands fleuves. *Hydrologie Continentale* **2**, 117–126.
- Junk W. J. (1997) General aspects of floodplain ecology with special reference to Amazonian floodplains. In *The Central-Amazonian Floodplain: Ecology of a Pulsing System, Ecological Studies* (ed. W. J. Junk). Springer Verlag, Heidelberg, Berlin, New York, pp. 3–22.
- Kim J.-H., Schouten S., Buscail R., Ludwig W., Bonnin J., Sinninghe Damsté J. S. and Bourrin F. (2006) Origin and distribution of terrestrial organic matter in the NW Mediterranean (Gulf of Lions): application of the newly developed BIT index. *Geochem. Geophys. Geosyst.* **7**, Q11017. <http://dx.doi.org/10.1029/2006GC001306>.
- Kim J.-H., Ludwig W., Schouten S., Kerhervé P., Herfort L., Bonnin J. and Sinninghe Damsté J. S. (2007) Impact of flood events on the transport of terrestrial organic matter to the ocean: a study of the Têt River (SW France) using the BIT index. *Org. Geochem.* **38**, 1593–1606.
- Kim J.-H., Buscail R., Bourrin F., Palanques A., Sinninghe Damsté J. S., Bonnin J. and Schouten S. (2009) Transport and depositional process of soil organic matter during wet and dry storms on the Têt inner shelf (NW Mediterranean). *Paleogeogr. Paleoclimatol. Paleoecol.* **273**, 228–238.
- Kim J.-H., Zarzycka B., Buscail R., Peters F., Bonnin J., Ludwig W., Schouten S. and Sinninghe Damsté J. S. (2010) Factors controlling the Branched Isoprenoid Tetraether (BIT) Contribution of river-borne soil organic carbon to the Gulf of Lions (NW Mediterranean). *Limnol. Oceanogr.* **55**, 507–518.
- Lal R. (2003) Soil erosion and the global carbon budget. *Environ. Int.* **29**, 437–450.
- LaZerte B. D. (1983) Stable carbon isotope ratios: implications for the source sediment carbon and for phytoplankton carbon

- assimilation in Lake Memphremagog, Quebec. *Can. J. Fish. Aquat. Sci.* **40**, 1658–1666.
- Lee S. and Furhman J. D. (1987) Relationships between biovolume and biomass of naturally derived marine bacterioplankton. *Appl. Environ. Microbiol.* **53**, 1298–1303.
- Lengger S. K., Hopmans E. C., Sinninghe Damsté J. S. and Schouten S. (2012) Comparison of extraction and work up techniques for analysis of core and intact polar tetraether lipids from sedimentary environments. *Org. Geochem.* **47**, 34–40.
- Likens G. E., Mackenzie F. T., Richey J. E., Sedell J. R. and Turekian K. K. (1981) Flux of organic carbon by rivers to the ocean. U S Dept Energy, NRC-C0NF-8009140, Washington, DC. p. 397.
- Loomis S. E., Russell James. M. and Sinninghe Damsté J. S. (2011) Distributions of branched GDGTs in soils and lake sediments from western Uganda: implications for a lacustrine paleothermometer. *Org. Geochem.* **42**, 739–751.
- Ludwig W., Probst J.-L. and Kempe S. (1996) Predicting the oceanic input of organic carbon by continental erosion. *Global Biogeochem. Cycles* **10**, 23–42.
- Mariotti A., Gadel F., Giresse P. and Mouzeo K. (1991) Carbon isotope composition and geochemistry of particulate organic matter in the Congo River (Central Africa): application to the study of Quaternary sediments off the mouth of the river. *Chem. Geol.* **86**, 345–357.
- Martinelli L. A., Victoria R. L., Forsberg B. R. and Richey J. E. (1994) Isotopic composition of major carbon reservoirs in the Amazon floodplain. *Int. J. Ecol. Environ. Sci.* **20**, 31–46.
- Martinelli L. A., Victoria R. L., de Camargo P. B., de Cassia Piccolo M., Mertes L., Richey J. E., Devol A. H. and Forsberg B. R. (2003) Inland variability of carbon–nitrogen concentrations and $\delta^{13}\text{C}$ in Amazon floodplain (várzea) vegetation and sediment. *Hydrol. Process.* **17**, 1419–1430.
- Martinez J. M. and Le Toan T. (2007) Mapping of flood dynamics and spatial distribution of vegetation in the Amazon floodplain using multitemporal SAR data. *Remote Sens. Environ.* **108**, 209–223.
- Martinez J. M., Guyot J. L., Filizola N. and Sondag F. (2009) Increase in suspended sediment discharge of the Amazon River assessed by monitoring network and satellite data. *Catena* **79**, 257–264.
- Mayorga E., Aufdenkampe A. K., Masiello C. A., Krusche A. V., Hedges J. I., Quay P. D., Richey J. E. and Brown T. A. (2005) Young organic matter as a source of carbon dioxide outgassing from Amazonian rivers. *Nature* **436**, 538–541.
- Meade R. H., Dunne T., Richey J. E., Santos U. M. and Salati E. (1985) Storage and remobilization of suspended sediment in the lower Amazon River of Brazil. *Science* **228**, 488–490.
- Meybeck M. (1982) Carbon, nitrogen, and phosphorus transport by world rivers. *Am. J. Sci.* **282**, 401–450.
- Meyers P. A. (1994) Preservation of elemental and isotopic source identification of sedimentary organic matter. *Chem. Geol.* **114**, 289–302.
- Molinier M., Guyot J. L., Oliveira E. and Guimaraes V. (1996) Les regimes hydrologiques de l'Amazonie et de ses affluents. In *L'hydrologie tropicale: geoscience et outil pour le developpement* (eds. P. Chevallier and B. Pouyaud). AIHS, Paris, pp. 209–222.
- Moreira-Turcq P., Seyler P., Guyot J. L. and Etcheber H. (2003) Exportation of organic carbon from the Amazon River and its main tributaries. *Hydrol. Process.* **17**, 1329–1344.
- Mortillaro J. M., Abril G., Moreira-Turcq P., Sobrinho R. L., Perez M. and Meziane T. (2011) Fatty acid and stable isotope ($\delta^{13}\text{C}$, $\delta^{15}\text{N}$) signatures of particulate organic matter in the Lower Amazon River: seasonal contrasts and connectivity between floodplain lakes and the mainstem. *Org. Geochem.* **42**, 1159–1168.
- Mounier S., Braucher R. and Benaim J. Y. (1998) Differentiation of organic matter's properties of the Rio Negro basin by cross flow ultra-filtration and UV-spectrofluorescence. *Water Res.* **33**, 2363–2373.
- New M., Lister D., Hulme M. and Makin I. (2002) A high-resolution data set of surface climate over global land areas. *Clim. Res.* **21**, 1–25.
- Nores M. (2011) The western Amazonian boundary for avifauna determined by species distribution patterns and geographical and ecological features. *Int. J. Ecol.* **2011**. <http://dx.doi.org/10.1155/2011/958684>.
- Oppermann B. I., Michaelis W., Blumenberg M., Frerichs J., Schulz H. M., Schippers A., Beaubien S. E. and Krüger M. (2010) Soil microbial community changes as a result of long-term exposure to a natural CO_2 vent. *Geochim. Cosmochim. Acta* **74**, 2697–2716.
- Pancost R. D. and Sinninghe Damsté J. S. (2003) Carbon isotopic compositions of prokaryotic lipids as tracers of carbon cycling in diverse settings. *Chem. Geol.* **195**, 29–58.
- Patterson B. D., Stotz D. F., Solari S., Fitzpatrick J. W. and Pacheco V. (1998) Contrasting patterns of elevational zonation for birds and mammals in the Andes of southeastern Peru. *J. Biogeography* **25**, 593–607.
- Pitcher A., Hopmans E. C., Mosier A. C., Park S.-J., Rhee S.-K., Francis C. A., Schouten S. and Sinninghe Damsté J. S. (2011) Core and intact polar glycerol dibiphytanyl glycerol tetraether lipids of ammonia-oxidizing archaea enriched from marine and estuarine sediments. *Appl. Environ. Microbiol.* **77**, 3468–3477.
- Quay P. D., Wilbur D. O., Richey J. E., Hedges J. I. and Devol A. H. (1992) Carbon cycling in the Amazon River: implications from the ^{13}C composition of particulate and dissolved carbon. *Limnol. Oceanogr.* **37**, 857–871.
- Raymond P. A. and Bauer J. E. (2001) Riverine export of aged terrestrial organic matter to the North Atlantic Ocean. *Nature* **409**, 497–500.
- Schlesinger W. H. and Melack J. M. (1981) Transport of organic carbon in the world's rivers. *Tellus* **33**, 172–187.
- Schouten S., Hugué C., Hopmans E. C., Kienhuis M. and Sinninghe Damsté J. S. (2007) Analytical methodology for TEX_{86} paleothermometry by high-performance liquid chromatography/atmospheric pressure chemical ionization-mass spectrometry. *Anal. Chem.* **79**, 2940–2944.
- Schouten S., Baas M., Hopmans E. C. and Sinninghe Damsté J. S. (2008) An unusual isoprenoid tetraether lipid in marine and lacustrine sediments. *Org. Geochem.* **39**, 1033–1038.
- Silva T. S. F., Costa M. P. F. and Melack J. M. (2009) Annual net primary production of macrophytes in the eastern Amazon floodplain. *Wetlands* **29**, 747–775.
- Sinninghe Damsté J. S., Hopmans E. C., Pancost R. D., Schouten S. and Geenevasen J. A. J. (2000) Newly discovered non-isoprenoid glycerol dialkyl glycerol tetraether lipids in sediments. *Chem. Comm.* **17**, 1683–1684.
- Sinninghe Damsté J. S., Hopmans E. C., Schouten S., Van Duin A. C. T. and Geenevasen J. A. J. (2002) Crenarchaeol: the characteristic core glycerol dibiphytanyl glycerol tetraether membrane lipid of cosmopolitan pelagic crenarchaeota. *J. Lipid Res.* **43**, 1641–1651.
- Sinninghe Damsté J. S., Ossebaer J., Abbas B., Schouten S. and Verschuren D. (2009) Fluxes and distribution of tetraether lipids in an equatorial African lake: constraints on the application of the TEX_{86} palaeothermometer and BIT index in lacustrine settings. *Geochim. Cosmochim. Acta* **73**, 4232–4249.
- Sinninghe Damsté J. S., Rijpstra W. I. C., Hopmans E. C., Weijers J. W. H., Foesel B. U., Jörg Overmann J. and Dedysh S. N. (2011) 13,16-Dimethyl octacosanedioic acid (isodiabolic acid): a

- common membrane-spanning lipid of Acidobacteria subdivisions 1 and 3. *Appl. Environ. Microbiol.* **77**, 4147–4154.
- Sioli H. (1950) Das Wasser in Amazonasgebiet. *Forsch. Fortsch.* **26**, 274–280.
- Spang A., Hatzepichler R., Brochier-Armanet C., Rattei T., Tischler P., Spieck E., Streit W., Stahl D. A., Wagner M. and Schleper C. (2010) Distinct gene set in two different lineages of ammoniaoxidizing archaea supports the phylum Thaumarchaeota. *Trends Microbiol.* **18**, 331–340.
- Spitzky A. and Ittekkot V. (1991) Dissolved and particulate organic matter in rivers. In *Ocean Margin in Global Change* (eds. R. F. C. Mantoura, J. M. Martin and R. Wollast). John Wiley and Sons, New York, pp. 5–17.
- Sun Q., Chu G., Liu M., Xie M., Li S., Ling Y., Wang X., Shi L., Jia G. and Lü H. (2011) Distributions and temperature dependence of branched glycerol dialkyl glycerol tetraethers in recent lacustrine sediments from China and Nepal. *J. Geophys. Res.* **116**, G01008. <http://dx.doi.org/10.1029/2010JG001365>.
- Tierney J. E. and Russell J. M. (2009) Distributions of branched GDGTs in a tropical lake system: implications for lacustrine application of the MBT/CBT paleoproxy. *Org. Geochem.* **40**, 1032–1036.
- Tierney J. E., Russell J. M., Eggermont H., Hopmans E. C., Verschuren D. and Sinninghe Damsté J. S. (2010) Environmental controls on branched tetraether lipid distributions in tropical East African lake sediments. *Geochim. Cosmochim. Acta* **74**, 4902–4918.
- Tyler J. J., Nederbragt A. J., Jones V. J. and Thurow J. W. (2010) Assessing past temperature and soil estimates from bacterial tetraether membrane lipids: evidence from the recent lake sediments of Lochnagar. *Scotland. J. Geophys. Res.* **115**, G01015. <http://dx.doi.org/10.1029/2009JG001109>.
- Volkoff B. and Cerri C. C. (1987) Carbon isotopic fractionation in subtropical Brazilian grassland soils: comparison with tropical forest soils. *Plant and Soil* **102**, 27–31.
- Walsh E. M., Ingalls A. E. and Keil R. G. (2008) Sources and transport of terrestrial organic matter in Vancouver Island fjords and the Vancouver-Washington Margin: a multiproxy approach using $\delta^{13}\text{C}_{\text{org}}$, lignin phenols, and the ether lipid BIT index. *Limnol. Oceanogr.* **53**, 1054–1063.
- Weijers J. W. H., Schouten S., van der Linden M., van Geel B. and Sinninghe Damsté J. S. (2004) Water table related variations in the abundance of intact archaeal membrane lipids in a Swedish peat bog. *FEMS Microbiol. Lett.* **239**, 51–56.
- Weijers J. W. H., Schouten S., Hopmans E. C., Geenevasen J. A. J., David O. R. P., Coleman J. M., Pancost R. D. and Sinninghe Damsté J. S. (2006a) Membrane lipids of mesophilic anaerobic bacteria thriving in peats have typical archaeal traits. *Environ. Microbiol.* **8**, 648–657.
- Weijers J. W. H., Schouten S., Spaargaren O. and Sinninghe Damsté J. S. (2006b) Occurrence and distribution of tetraether membrane lipids in soils: implications for the use of the TEX₈₆ proxy and the BIT index. *Org. Geochem.* **37**, 1680–1693.
- Weijers J. W. H., Schouten S., van den Donker J. C., Hopmans E. C. and Sinninghe Damsté J. S. (2007) Environmental controls on bacterial tetraether membrane lipid distribution in soils. *Geochim. Cosmochim. Acta* **71**, 703–713.
- Weijers J. W. H., Panoto E., van Bleijswijk J., Schouten S., Rijpstra W. I. C., Balk M., Stams A. J. M. and Sinninghe Damsté J. S. (2009a) Constraints on the biological source(s) of the orphan branched tetraether membrane lipids. *Geomicrobiol. J.* **26**, 402–414.
- Weijers J. W. H., Schouten S., Schefuß E., Schneider R. R. and Sinninghe Damsté J. S. (2009b) Disentangling marine, soil and plant organic carbon contributions to continental margin sediments: a multi-proxy approach in a 20,000 year sediment record from the Congo deep-sea fan. *Geochim. Cosmochim. Acta* **73**, 119–132.
- Weijers J. W. H., Wiesenberg G. L. B., Bol R., Hopmans E. C. and Pancost R. D. (2010) Carbon isotopic composition of branched tetraether membrane lipids in soils suggests a rapid turnover and a heterotrophic life style of their source organism(s). *Biogeosciences* **7**, 2959–2973.
- Young K. R. and Blanca L. (1999) Peru's humid eastern montane forests: An overview of their physical settings, biological diversity, human use and settlement, and conservation needs. DIVA Technical Report 5, Kalø, Denmark, Centre for Research on Cultural and Biological Diversity of Andean Rainforests (DIVA), 97 p.
- Zhu C., Weijers J. W. H., Wagner T., Pan J.-M., Chen J.-F. and Pancost R. D. (2011) Sources and distributions of tetraether lipids in surface sediments across a large river-dominated continental margin. *Org. Geochem.* **42**, 376–386.
- Zink K. G., Vandergoes M. J., Mangelsdorf K., Dieffenbacher-Krall A. C. and Schwark L. (2010) Application of bacterial glycerol dialkyl glycerol tetraethers (GDGTs) to develop modern and past temperature estimates from New Zealand lakes. *Org. Geochem.* **41**, 1060–1066.
- Zocatelli R. O. (2010) Reconstrução paleoclimática do Lago Santa Nina e Lago Boqueirão. Ph.D. Thesis, Departamento de Geoquímica, Universidade Federal Fluminense, Niteroi, Brasil.

Associate editor: H. Rodger Harvey